

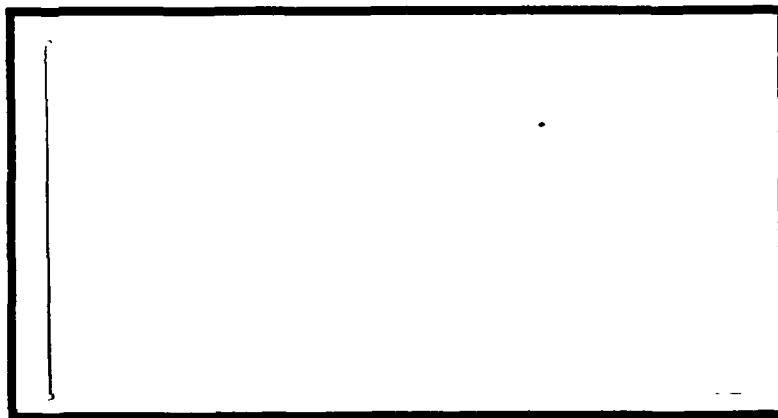
DTIC FILE COPY

(1)

AD-A203 176



DTIC  
ELECTE  
JAN 17 1989  
S H D



DEPARTMENT OF THE AIR FORCE  
AIR UNIVERSITY

**AIR FORCE INSTITUTE OF TECHNOLOGY**

Wright-Patterson Air Force Base, Ohio

**DISTRIBUTION STATEMENT A**

Approved for public release;  
Distribution Unlimited

89 1 17 029

AFIT/GAE/AA/88D-22

INCOMPRESSIBLE FLOW FRICTION  
COEFFICIENTS IN A SIMULATED HEAT PIPE

THESIS

David A. Manley  
Captain, USAF

AFIT/GAE/AA/88D-22

DTIC  
ELECTE  
JAN 17 1989  
S H D

Approved for public release; distribution unlimited

AFIT/GAE/AA/88D-22

INCOMPRESSIBLE FLOW FRICTION COEFFICIENTS  
IN A SIMULATED HEAT PIPE

THESIS

Presented to the Faculty of the School of Engineering  
of the Air Force Institute of Technology

Air University

In Partial Fulfillment of the  
Requirements for the Degree of  
Master of Science in Aeronautical Engineering

David A. Manley, B.S.

Captain, USAF

December 1988

Approved for public release; distribution unlimited.

### Acknowledgements

In performing the experimentation and writing of this thesis, I have had a great deal of support from others. With much gratitude, I wish to thank my faculty advisor, Dr. James Hitchcock, for his keen and perceptive insight. He should be praised as a thesis advisor. Without his guidance, this effort would not have been completed on time. I also wish to thank Jay Anderson for his assistance in acquiring data. A word of thanks also goes to my wife, [REDACTED] for all the sacrifices she made and for her understanding and support during the most difficult time of our life. Finally, I wish to thank my children, [REDACTED] [REDACTED] who have faithfully loved their "studying" Dad. I sure look forward to spending "quantity" time with them for a change.

David A. Manley



Accession For	
NTIS GRA&I	<input checked="checked" type="checkbox"/>
DTIC TAB	<input type="checkbox"/>
Unannounced	<input type="checkbox"/>
Justification	
By	
Distribution/	
Availability Codes	
Dist	Avail and/or Special
A-1	

## Table of Contents

	Page
Acknowledgements . . . . .	ii
List of Figures . . . . .	iv
Notation . . . . .	v
Abstract . . . . .	vii
I. Introduction . . . . .	1-1
Literature Review . . . . .	1-1
Laminar Flow in a Porous Tube	
With Blowing . . . . .	1-2
Laminar Flow in a Porous Tube	
With Suction . . . . .	1-5
Flows Simulating Heat Pipe	
Operation . . . . .	1-9
Objective and Scope . . . . .	1-11
II. Experimental Model . . . . .	2-1
Porous Pipe . . . . .	2-1
Pressure Taps . . . . .	2-3
Pressure Measurements . . . . .	2-3
Data Acquisition . . . . .	2-5
III. Numerical Model . . . . .	3-1
Governing Equations . . . . .	3-1
Solution Method . . . . .	3-5
IV. Discussion of Results . . . . .	4-1
V. Conclusions and Recommendations . . . . .	5-1
Conclusions . . . . .	5-1
Recommendations . . . . .	5-1
Appendix A: Raw Experimental Pressure Data . . . . .	A-1
Appendix B: Numerical Simulation Code . . . . .	B-1
Appendix C: Numerical Printouts . . . . .	C-1
Bibliography . . . . .	BIB-1
Vita . . . . .	VITA-1

# List of Figures

Figure		Page
2-1	Experimental Test Configuration . . . . .	2-2
2-2	Pressure Tap Distribution . . . . .	2-4
2-3	Porous Pipe Calibration Results . . . . .	2-8
3-1	Element of Fluid for Equation of Motion .	3-1
3-2	Element of Fluid Used for Mass Balance .	3-3
4-1	Experimental Variation of Radial Reynolds Number With Axial Location Along Porous Pipe . . . . .	4-2
4-2	Experimental Variation of Wall Static Pressure With Axial Location Along Porous Pipe . . . . .	4-3
4-3	Curve Fit of Quaile and Levy's Prediction of Separation for Constant Wall Suction and Parabolic Inlet Velocity Profile . . . .	4-5
4-4	Evaporator (Blowing) Friction Coefficient Results . . . . .	4-6
4-5	Curve Fit of Kinney's Universal Law of Wall Friction for Fully-Developed Laminar Flow in Porous Tubes and Average Condenser Values From This Experiment . . . . .	4-8

### Notation

A	porous pipe property used in Equation 2-3	$\left( \frac{\text{lb}_f - \text{ft}}{\text{sec}} \right)$
$A_c$	pipe cross-sectional area	$(\text{ft}^2)$
$A_p$	pipe wall perimeter area	$(\text{ft}^2)$
D	pipe diameter	$(\text{ft})$
f	friction coefficient	(Eq 3-3)
$f^*$	impermeable wall friction coefficient	
$\bar{f}_c$	average condenser friction coefficient	(Eq 3-16)
$F_c$	axial force acting on condenser	(Eq 3-15)
$g_c$	conversion factor	$\left( \frac{\text{lb}_m - \text{ft}}{\text{lb}_f - \text{sec}^2} \right)$
L	pipe length	$(\text{ft})$
M	Mach number	
$\dot{m}$	mass flow rate	$\left( \frac{\text{lb}_m}{\text{sec}} \right)$
P	pressure	$\left( \frac{\text{lb}_f}{\text{ft}^2} \right)$
R	ideal gas constant for air	$\left( \frac{\text{lb}_f - \text{ft}}{\text{lb}_m - ^\circ\text{R}} \right)$
$Re_w$	radial Reynolds number	(Eq 3-14)
$Re_x$	axial Reynolds number	(Eq 3-13)
T	temperature	$(^\circ\text{R})$
$\bar{U}$	average axial velocity	$(\text{ft}/\text{sec})$
$V_w$	radial velocity at wall	$(\text{ft}/\text{sec})$

X	axial location (ft)
$\Delta(P^2)$	difference in square of pressures across pipe wall $\left(\frac{\text{lb}_f^2}{\text{ft}^4}\right)$
$\Delta W$	change in momentum ( $\text{lb}_f$ )
$\Delta X$	axial increment (ft)
$\phi$	momentum flux factor (Eq 1-1)
$\gamma$	ratio of specific heats
$\mu$	dynamic viscosity $\left(\frac{\text{lb}_f - \text{sec}}{\text{ft}^2}\right)$
$\nu$	momentum diffusivity ( $\text{ft}^2/\text{sec}$ )
$\rho$	density $\left(\frac{\text{lb}_m}{\text{ft}^3}\right)$
$\rho V_w$	mass flux $\left(\frac{\text{lb}_f - \text{sec}}{\text{ft}^2}\right)$
$\tau_w$	wall shear stress $\left(\frac{\text{lb}_f}{\text{ft}^2}\right)$
$\xi$	dimensionless axial velocity (Eq 2-1)

Superscripts and Subscripts:

CE	condenser entrance
D	end of the condenser
LE	end of the evaporator
U	beginning of the evaporator
1	upstream end of the $\Delta X$ increment
2	downstream end of the $\Delta X$ increment



Abstract

This thesis examines the combined effects of pressure gradients and blowing and suction on frictional forces in a heat pipe with relatively low radial Reynolds numbers. A porous tube is used to simulate the heat pipe and a vacuum pump is used to generate the air flow. By measuring the static pressure variation along the pipe wall and using a one-dimensional, incompressible, numerical model, the frictional forces are obtained and compared to laminar fully-developed theoretical values. Four flow rate cases with radial Reynolds numbers of 1.8, 3.5, 6.5, and 12.6 were studied. In this range, the flow in the evaporator was fully-developed. In the condenser, however, the fully-developed solution consistently under predicted the average condenser friction coefficient. Deviation from the fully-developed solution increased as the flow rate increased.

# INCOMPRESSIBLE FLOW FRICTION COEFFICIENTS IN A SIMULATED HEAT PIPE

## I. Introduction

The purpose of this chapter is twofold. First, a review of past efforts, both analytical and experimental, which studied flow conditions in porous constant diameter circular cylinders with mass transfer at the walls will be made. This review will provide a framework for understanding the results of this investigation in addition to providing sources for comparison. Second, the objective and scope of this study will be outlined.

## Literature Review

Examining fluid flow in porous tubes has proven to be an excellent way of understanding the combined effects of pressure gradients and blowing and suction on frictional forces in heat pipes. Most investigators have concentrated on the effects of either blowing or suction separately. For this reason, the literature discussed will be separated into 1) laminar flow in a porous tube with blowing, 2) laminar flow in a porous tube with suction, and 3) flows simulating heat pipe operation.

Laminar Flow in a Porous Tube With Blowing. Berman (1) was the first to solve the Navier-Stokes equations for steady, fully-developed, incompressible, laminar flow in a porous tube with uniform injection. He observed that fluid injection through the pipe walls has a noticeable effect on velocity profiles and pressure gradients. He showed that blowing in all cases would cause the pressure to decrease in the direction of axial flow. He also found that blowing would flatten the velocity profile at the center of the pipe and increase the slope of the profile at the pipe wall.

Kinney (2) using a numerical solution to the boundary-layer equation, showed that for fully-developed laminar pipe flow with either uniform blowing or suction, the product of the friction coefficient,  $f$ , and axial Reynolds number,  $Re_x$  is only a function of the radial Reynolds number,  $Re_w$ . He termed this relationship "the universal law of wall friction." With no blowing nor suction,  $f \cdot Re_x = 16$ . He further noted that this product increases with blowing and decreases with suction. Kinney also discussed the importance of a parameter he termed "the momentum flux factor," which is defined as

$$\phi = \frac{\overline{U^2}}{(\bar{U})^2} \quad (1-1)$$

This parameter provides an indication of the relative flatness of the velocity profile. For the impossible case

of slug flow,  $\phi$  would equal unity, while for the impermeable wall case in fully-developed laminar pipe flow,  $\phi$  is equal to 1.33. For increasing blowing rates, which have flatter velocity profiles,  $\phi$  decreases asymptotically to 1.2337. Finally, Kinney verified that "for a given axial Reynolds number, blowing increases the wall friction." This is opposite to that found for flat-plate boundary-layer flows for which the wall friction is reduced by fluid injection normal to the wall. The reason for this is that for boundary-layer flow over a flat-plate at zero incidence, the axial pressure gradient is zero, even in the presence of uniform blowing normal to the plate surface. Here, blowing decreases the slope of the velocity profile at the surface resulting in less wall friction. For the pipe flow with blowing, the axial pressure gradient is negative to provide the force required for axial acceleration. As the magnitude of the pressure gradient increases with blowing, the slope of the velocity profile near the wall increases. The end result is greater wall friction.

The first attempt to verify experimentally the similarity solutions for fully-developed laminar flow in a porous pipe with wall injection was performed by Bundy and Weissberg (3). They were able to confirm the negative axial pressure gradients predicted by Berman.

Gupta (4) studied the effect of blowing on the laminar flow in the inlet region of a tube. His interest was in

controlling the length of the inlet region. Because blowing increases boundary-layer growth, his proposal was to use blowing as the controlling device. His analysis assumed steady, laminar flow of an incompressible Newtonian fluid entering a circular tube with a constant uniform velocity. The same fluid was injected into the flow, normal to the wall at a constant velocity. He found that as the blowing  $Re_w$  increased, the axial distance required for the attainment of a fully-developed flow solution decreased. He also found that for a given blowing  $Re_w$ , the length required to achieve the fully-developed solution decreases as the inlet axial Reynolds number is decreased. This fact when applied to heat pipes, where the flow begins in the evaporator with no axial velocity, allows the hydrodynamic entrance length in the evaporator to be ignored for even extremely small evaporation rates.

Bowman (5), determined experimentally that transition is retarded due to mass injection. He found that the flow remains laminar, when blowing is present, up to axial Reynolds numbers on the order of  $10^6$ . Combining Gupta's observation that, with blowing, fully-developed laminar flow is quickly achieved with Bowman's observation that, with blowing, the flow remains fully-developed and laminar provides an insight as to why flow with blowing is relatively well behaved compared to flow with suction.

Laminar Flow in a Porous Tube With Suction. Berman (1)

showed that, for fully-developed laminar flow, relatively small amounts of suction can lead to a pressure rise in the axial flow direction. In the presence of suction at the wall, the decrease in axial momentum tends to cause an increase in pressure in the flow direction, while the wall shear tends to decrease the pressure. He demonstrated that changes in the familiar parabolic velocity profile observed in tubes with impermeable walls are much more pronounced when fluid is removed through the system boundary than when fluid is injected. For small suction, the centerline value of the velocity increases and the slope of the profile at the wall decreases. Because the velocity of the fluid near the wall is small, it is affected more by the adverse pressure gradient. As suction increases, the velocity gradient at the wall approaches zero resulting in a typical separation profile. He also noted that the amount of suction required to produce a separation profile is very small, (on the order of  $Re_w = 4$ ). Moreover, he showed that this phenomena is independent of  $Re_x$ . In contrast, for external flows, where the pressure gradient is not dependent on the suction rate, suction actually stabilizes the flow.

In this region of instability Berman (1) made his most interesting discoveries. He noticed several peculiarities with his numerical similar solutions. First when  $4.1 < Re_w < 4.6$ , there are two similar solutions for the ratio of

maximum to average axial velocity, (similar in the sense that the shapes of the velocity profiles do not vary with distance along the pipe). He felt only one of the solutions had any physical significance and that transition to turbulent flow would occur before the second solution could ever be achieved. More importantly, when he sought similar solutions for  $Re_w$  between the range of 4.6 and about 18, he found that none existed. For  $Re_w$  greater than 18, he found additional multiple solution ranges corresponding to reverse flow in various regions of the flow between the wall and the centerline of the pipe. Berman did not expect the absence of solutions for  $Re_w$  between 4.6 and 18.

Weissberg (6) was the first to investigate the suction region identified by Berman as having a non-similar solution. It was Weissberg who first referred to this region as the "forbidden" range of suction rates. He dealt with the partial differential equation of motion for the pipe case when similarity of the solutions is not imposed. His main assumptions were steady, incompressible, axially-symmetric flow in a pipe with uniform suction. He simplified the general equation of motion for the limit of high axial Reynolds number. He concluded that the nonexistence of similar solutions is to be associated with a state of the flow field for which the entrance region extends all the way from the pipe inlet to the location where the axial velocity is reduced to zero by wall suction.

Weissberg's analysis narrowed this region to  $4.8188 < Re_w < 15.2688$ .

Kinney (2) also found that, for suction of a fully-developed laminar flow, wall friction decreases with increasing  $Re_w$ . He established the limit for  $Re_w$  which would cause the wall friction to be reduced to zero at no less than 4.626. The last calculation he carried out was for  $Re_w = 4.618$ . This can be compared to Berman's original estimate of 4.6.

Kinney also provided values for the fully-developed laminar  $\phi$  when suction is present. He did not compute any  $\phi$ 's for  $Re_w > 4.618$ . For radial Reynolds numbers larger than this, fully-developed laminar flow does not exist. As suction increases from zero to the edge of the "forbidden" suction range, he showed  $\phi$  for fully-developed laminar flow increasing from 1.33 to approximately 1.9.

Raithby (7), using the same assumptions as Berman and Kinney, determined the range for which the wall friction becomes zero in fully-developed laminar flow to be between  $Re_w$  of 4.5978 and 4.5980. Raithby, like Berman, had multiple solutions for suction radial Reynolds numbers greater than the "forbidden" suction range. He felt that the velocity profile selected by the flow would depend on the inlet velocity profile. The most probable profile would likely transition to turbulent flow due to a combination of



velocity profile inflections and an opposing pressure gradient.

Hornbeck, Rouleau, and Osterle (8) developed a numerical model to examine the entrance region for a round pipe with any entrance velocity profile and any suction boundary condition including inertia effects. They limited their analysis to cases where the suction rates were small, (small values for the ratio of the mean suction velocity to the mean axial velocity). As in the previous uniform suction studies, they found that for moderate suction rates, the loss of axial momentum flux resulting from flow through the wall was only partially offset by the wall shear and the pressure rose in the axial direction. For very small suction rates, radial Reynolds numbers of approximately 2 and less, the effect of wall shear will be greater than that due to the loss of axial momentum flux, and the pressure will drop with axial distance. For uniform inlet velocities, they found that the pressure would decrease axially even more than with a fully-developed laminar parabolic inlet velocity profile. For the uniform inlet velocity profile case, if  $Re_w$  is sufficiently large, the pressure would first decrease for some axial distance and then begin to rise. Only when the high velocity gradient at the wall has decreased enough, does the loss of axial momentum by flow through the walls begin to have its effect on the pressure, causing it to rise.

The first to experiment in the "forbidden" range of suction were Quaile and Levy (9). They also performed an analysis assuming steady, laminar, incompressible flow in a constant diameter porous tube with uniform suction at the wall to compare with their experimental results. They measured the axial pressure variations and the velocity profiles of a silicone fluid entering a region of uniform suction with a parabolic velocity profile. For these conditions, their results were compatible with the earlier theories. Provided in their report is a figure showing theoretical axial locations where separation should occur for a given  $Re_w$ . For  $Re_w$  between 6 and 22, the measured separation locations occurred slightly later than predicted. For  $Re_w = 30$ , the measured separation location occurred slightly earlier than predicted.

Flows Simulating Heat Pipe Operation. Measurement of vapor dynamics in actual heat pipes presents many experimental difficulties. Because heat pipes are carefully sealed from their environment, it is difficult to determine the velocity profiles in the vapor region. Wageman and Guevara (10) were able to demonstrate that injecting a fluid through the walls over half the length of a porous pipe and then extracting the fluid through the walls over the second half of the porous pipe simulated the vapor dynamics in a heat pipe quite well. The mass injection at the wall simulates the evaporator and the mass extraction at the wall

simulates the condenser. For heat pipes, the velocity profile leaving the evaporator is somewhere between the parabolic and uniform velocity profiles and unless the adiabatic region is sufficiently long, the parabolic profile is never attained at the inlet of the condenser. Since Wageman and Guevara, other researchers such as Quaile and Levy, and Bowman have used a porous pipe to simulate a heat pipe.

Kinney (2) as mentioned previously, developed a relationship for the friction coefficient and axial Reynolds number product for various radial Reynolds numbers for fully-developed laminar flow. Bowman (5) modified this incompressible relationship, based on experimental data, to extend to compressible flow. For laminar flow, he found the relationship to be

$$f \cdot \text{Re}_x = 16 \left[ 1.2337 - 0.2337 e^{\left[ 0.0363 \text{Re}_w \right]} \right] e^{\left[ \frac{6M^2}{5} \right]} \quad (1-2)$$

For turbulent flow with axial Reynolds numbers less than 150,000 Kinney and Sparrow (11) suggested the following relationship

$$f = f^* \left[ 1 + 17.5 \text{Re}_x^{0.25} \left( \frac{V_w}{U} \right) \right] \quad (1-3)$$

where  $V_w$  is the radial velocity at the wall,  $\bar{U}$  is the average axial velocity, and  $f^*$ , the impermeable wall friction coefficient, may be estimated by the Blasius equation

$$f^* = \frac{0.079}{Re_x^{0.25}} \quad (1-4)$$

#### Objective and Scope

The primary objective of this research is to study the behavior of a simulated heat pipe operating at relatively low radial Reynolds numbers. To better understand this behavior, data from a simulated heat pipe will be processed with a one-dimensional, numerical model. To lower the radial Reynolds number via a lower density, air will be pulled through the porous tube with a vacuum pump instead of using compressed air upstream. The static pressure will be measured along the pipe wall. This pressure distribution becomes the input to a one-dimensional, incompressible, numerical model for a constant diameter porous tube with variable mass injection and extraction. The numerical model will provide the friction coefficient distribution in the evaporator as well as an average friction factor for the condenser. These friction coefficients will then be compared to the fully-developed solutions predicted by Kinney. Also, the measured axial separation locations will be compared to those predicted by Quaile and Levy.

## II. Experimental Model

The purpose of this study was to obtain static pressure data (axial pressure distribution) for flow inside a porous tube simulating a heat pipe at relatively low radial Reynolds numbers. The pressure measurements were used as input to a one-dimensional numerical model discussed in detail in Chapter 3. In this chapter, a description of the porous pipe, a discussion of the experimental set up, and the calibration results will be presented.

### Porous Pipe

Following the example of Bowman (5), an ultra high molecular weight polyethylene porous pipe was obtained from Porex Technologies, (PVC tube part # 5139). The pipe had an inside diameter of 0.5 inches and a wall thickness of 0.25 inches. The average pore size was 20 microns. The length used in the heat pipe simulation was 31.81 inches. The evaporator and condenser sections were both 15.66 inches long separated by an adiabatic, impermeable wall of 0.50 inches in length. Both ends were sealed with plastic caps to insure that all flow entering or leaving the pipe was through the pipe walls. Half of the pipe was then placed into a vacuum tank, with the opposite half exposed to ambient air (see Figure 2-1). A portable shop vacuum pump connected to the vacuum tank generated the flow.

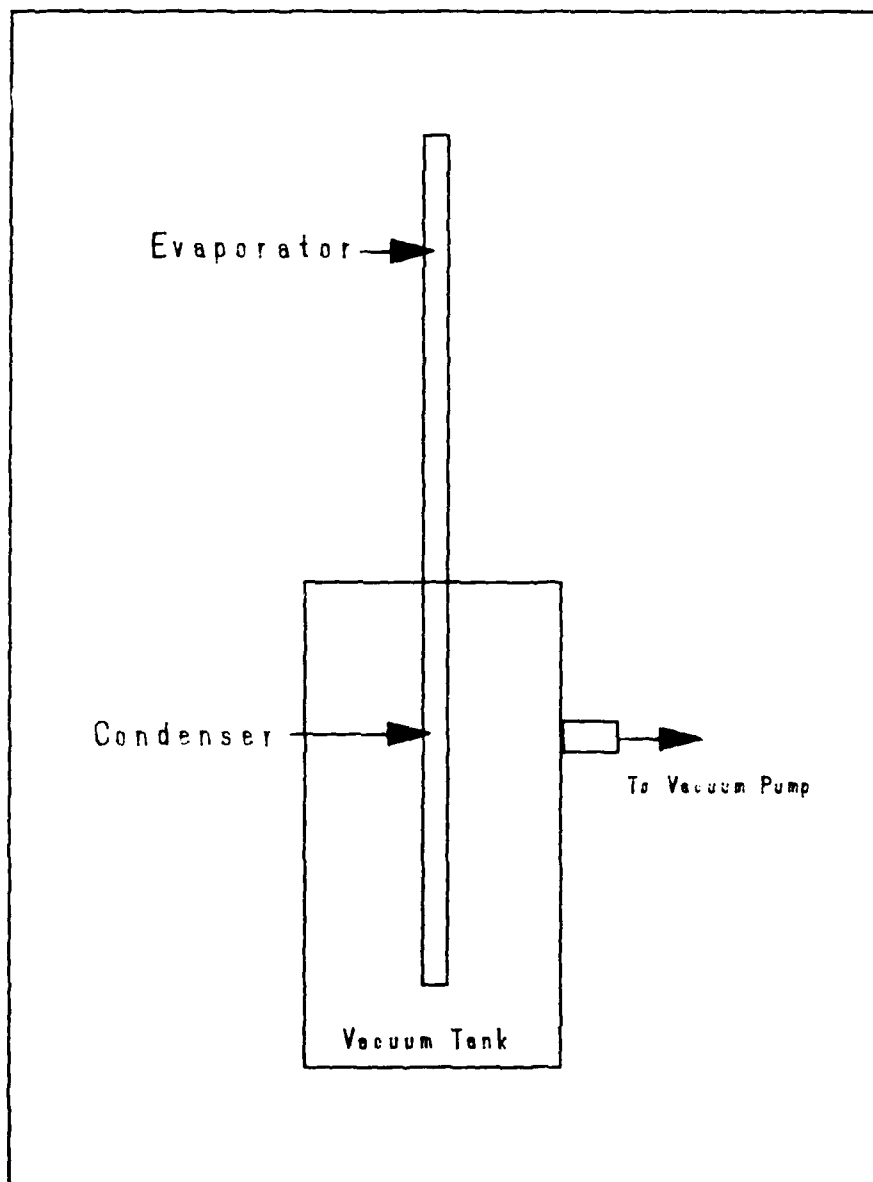


Figure 2-1. Experimental Test Configuration

### Pressure Taps

Thirty pressure taps were installed in the porous pipe by cementing 0.5 inch long 0.060 inch outside diameter stainless steel tubes into 0.058 inch outside diameter holes drilled in the tube. This produced a snug fit. The stainless steel tube was inserted in the porous pipe so that its end was flush with the inside wall of the pipe. Two of the thirty pressure taps were installed through the end caps to obtain pressure measurements for  $\xi = 0.0$  and  $\xi = 1.0$  where  $\xi$ , the dimensionless axial location, is defined as

$$\xi = \frac{X}{L} \quad (2-1)$$

The remaining twenty eight pressure taps were distributed axially along the pipe, eleven in the evaporator and seventeen in the condenser (see Figure 2-2), with their axial locations documented in the numerical code found in Appendix B.

### Pressure Measurements

All pressure measurements were made using a T-type Scanivalve, from Scanivalve Corporation. A Robinson Halpern model 157B-W020D-F-V31 differential pressure transducer with a pressure range of  $\pm 0-2$  inches of water producing an output of  $\pm 1$  volt was used in the Scanivalve. The system allowed for 36 pressure measurements with the one pressure transducer. Two of the six remaining scanivalve ports were

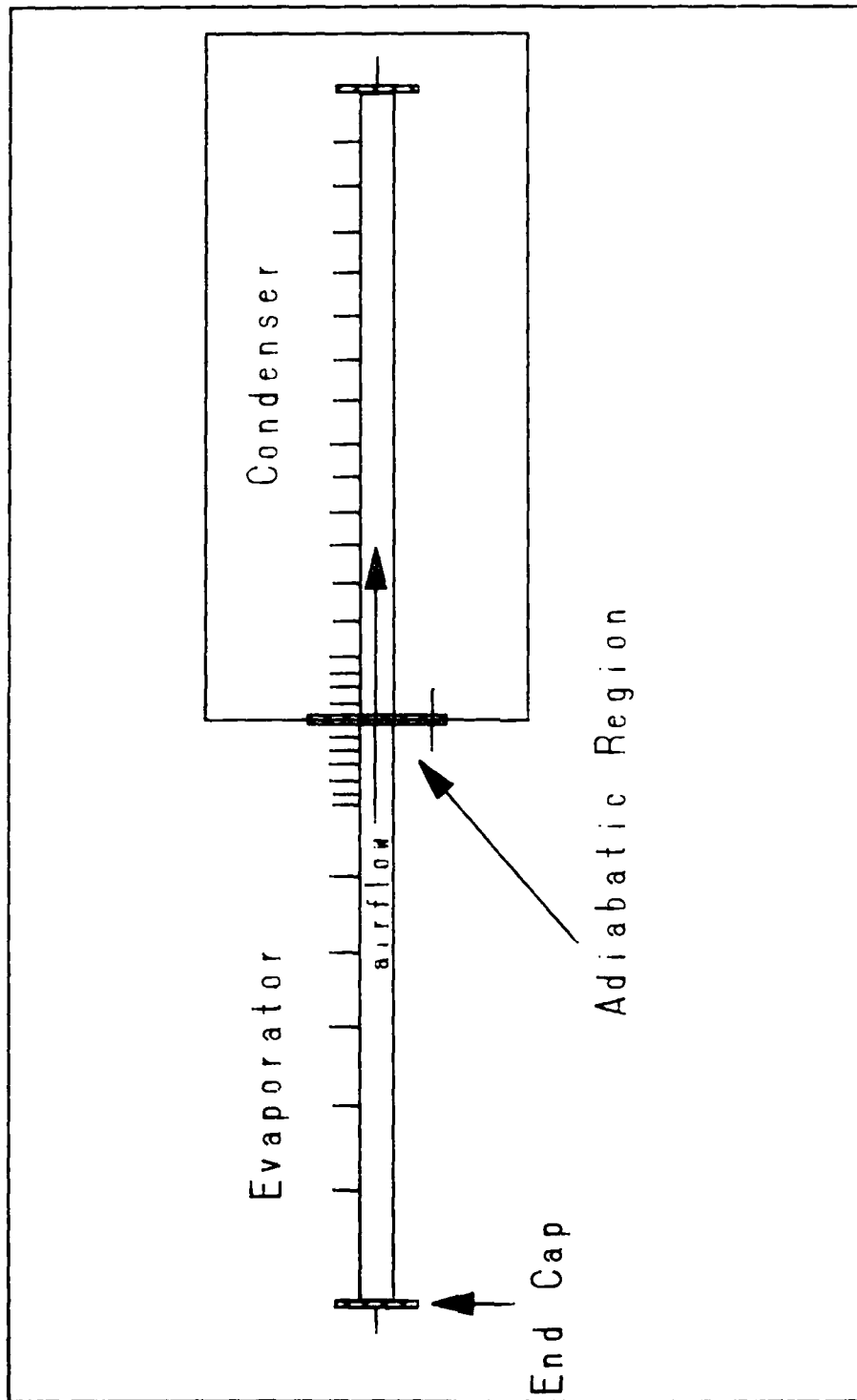


Figure 2-2. Pressure Tap Distribution



used to measure the pressure in the vacuum tank and the ambient pressure. For the three lowest flow rate cases, all pressure differences were measured with respect to ambient pressure. For the highest flow rate case, all pressure differences were measured with respect to the pressure port immediately leaving the evaporator. To obtain absolute pressures, the ambient pressure was measured with a barometer. The main disadvantage of the system was the amount of time required by the transducer's diaphragm to reach a steady pressure reading. The pressure transducer was calibrated using an inclined water manometer as the standard.

#### Data Acquisition

Data acquisition was done via a Zenith Z-100 computer. Pressure transducer input into the computer was digitized through a Dual Systems Control model AIM12 analog-to-digital card in the computer. An offset option on the transducer and the card's amplification were set so signals from 0 to  $\pm 1$  volts could be read with a resolution of 0.04883 millivolts. Shielded cables were used to reduce noise introduced into the system. Noise was further reduced by averaging 1000 data samples for every pressure reading. To allow time for the transducer's diaphragm to reach equilibrium, a delay loop was used as the scan valve changed ports. Once the data had been read and averaged by the

computer, it was displayed on the monitor and stored on an electronic disk.

#### Pipe Calibration

In addition to the pressure distribution along the porous pipe, the numerical model required information regarding the resistance of the porous pipe to mass flux ( $\rho V_w$ ) through its walls. Muskat (12) showed using Darcy's Law that, for the flow of a compressible gas through a porous medium,  $\rho V_w$  can be related to the pressure difference across the porous medium by the expression

$$\Delta(P^2) = A(\rho V_w)^2 + B(\rho V_w) \quad (2-2)$$

where the constants A and B are properties of the medium. For all cases of this study, the mass flux rates were very small and the contribution of the  $A(\rho V_w)^2$  term was negligible. Muskat's relationship was therefore simplified to

$$\Delta(P^2) = B(\rho V_w) \quad (2-3)$$

To determine the constant B,  $\Delta(P^2)$  and  $\rho V_w$  were measured at various mass flow rates. The two 2 inch samples used during the calibration were obtained from opposite ends of the porous pipe used to simulate the heat pipe. Two pressure ports for each sample connected to a 50 inch U-tube water manometer were used to measure the average pressure difference across the sample walls. A 1 inch precision bore

"flowrator" with a range of 0.05 - 0.44 cfm was used to measure  $\rho V_w$ . The method used to measure  $\Delta(P^2)$  and  $\rho V_w$  was the same as outlined by Bowman (5) with the exception that flow was induced by a vacuum pump instead of compressed air. It was assumed that the temperature of the air entering the "flowrator" was the same as ambient. Using a least-squares technique to curve fit the experimental data shown in Figure 2-3, the constant B in Equation (2-2) was found to be  $3.592472958 \times 10^8 \frac{\text{lbf}}{\text{ft-sec}}$ . As can be seen in Figure 2-3, the bob indicator tended to stick to the walls of the "flowrator" at the lower flow rates. When calibrating sample 1, readings were taken from the lowest to highest flow rates. When calibrating sample 2, readings were reversed.

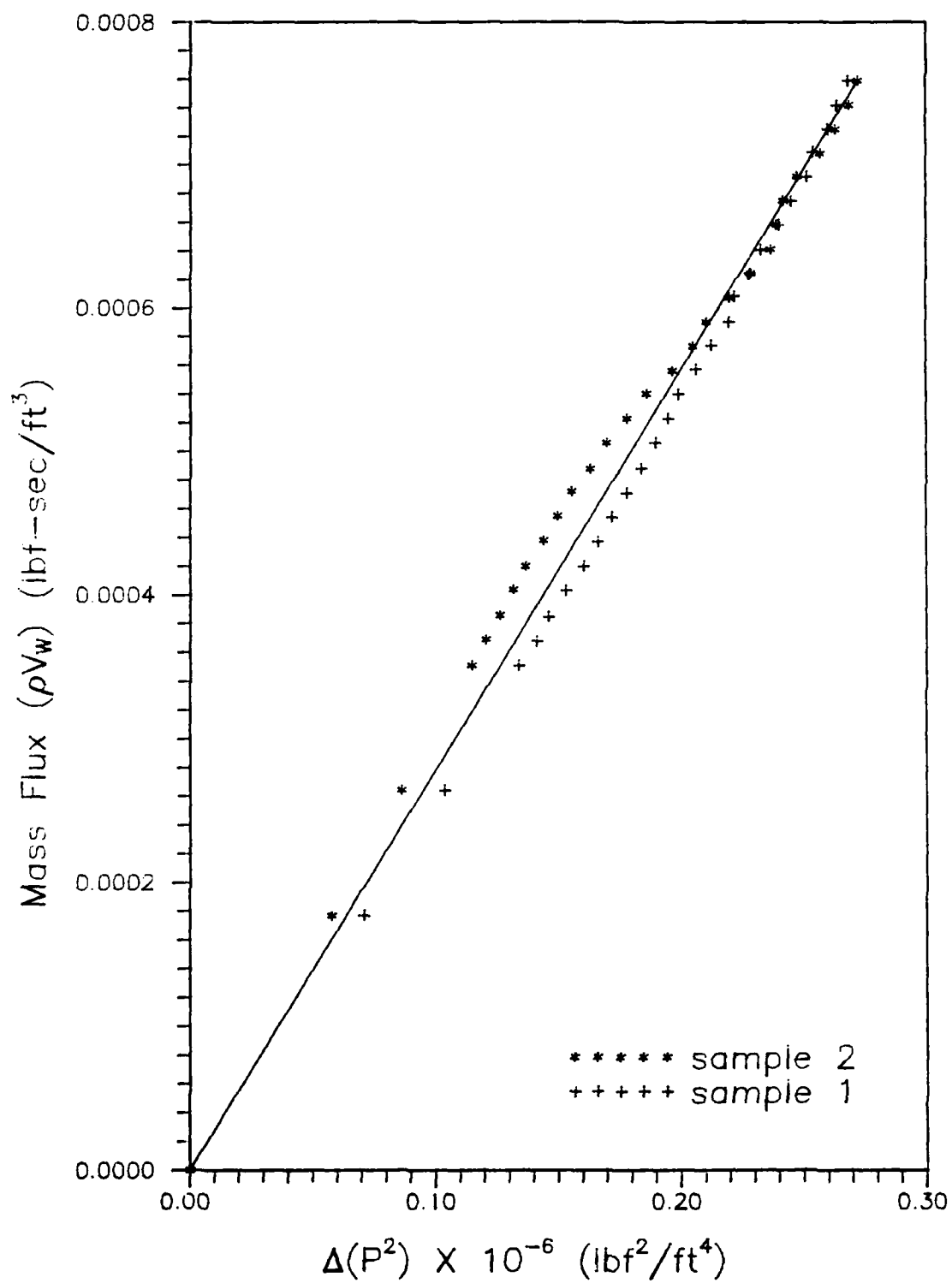


Figure 2-3. Porous Pipe Calibration Results.

### III. Numerical Model

This chapter describes the one-dimensional numerical model used to reduce the data measured during the experimental phase of the study. First, the governing equations used in solving the flow properties will be presented. Then, the solution technique will be described.

#### Governing Equations

One-dimensional, steady, adiabatic, incompressible flow was assumed for the model. In the numerical simulation code contained in Appendix B, a provision for compressible flow has been made following the example of Holladay (13). All flows evaluated in this study, however, are incompressible.

To approximate the shear stress at the pipe wall, Newton's second law was applied to an element of fluid in the pipe as shown in Figure 3-1.

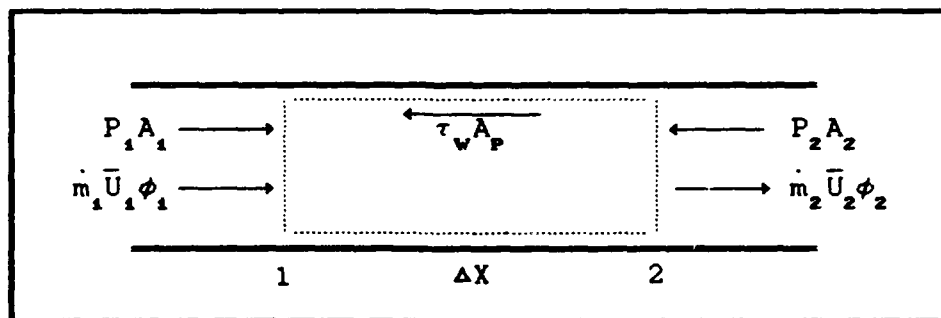


Figure 3-1. Element of Fluid for Equation of Motion

Applying Newton's second law for steady flow to the fluid element gives

$$\frac{\dot{m}_2 \bar{U}_2 \phi_2}{g_c} - \frac{\dot{m}_1 \bar{U}_1 \phi_1}{g_c} = (P_1 A_1 - P_2 A_2) - \tau_w A_p \quad (3-1)$$

where  $A_p$  is the wall surface area for the increment  $\Delta X$ .

Solving for  $\tau_w$  gives

$$\tau_w = \frac{1}{A_p} \left[ \frac{\dot{m}_1 \bar{U}_1 \phi_1}{g_c} - \frac{\dot{m}_2 \bar{U}_2 \phi_2}{g_c} + (P_1 - P_2) A_c \right] \quad (3-2)$$

where  $A_c$  is the cross-sectional area equal to  $A_1$  and  $A_2$ . The friction coefficient is given by

$$f = \frac{2\tau_w g_c}{\rho \bar{U}^2} \quad (3-3)$$

where

$$\bar{U} = \frac{(\bar{U}_1 + \bar{U}_2)}{2} \quad (3-4)$$

Substituting the expression for  $\tau_w$  given by Equation (3-2) in Equation (3-3) gives an expression for the friction coefficient in terms of quantities which can be calculated from the input pressure distribution

$$f = \frac{2 [\Delta W + (P_1 - P_2) A_c] g_c}{\rho \bar{U}^2 A_p} \quad (3-5)$$

where

$$\Delta W = \frac{\dot{m}_1 \bar{U}_1 \phi_1}{g_c} - \frac{\dot{m}_2 \bar{U}_2 \phi_2}{g_c} \quad (3-6)$$

The average axial velocities along the pipe were calculated from a mass balance on an element of fluid in the pipe as seen in Figure 3-2.

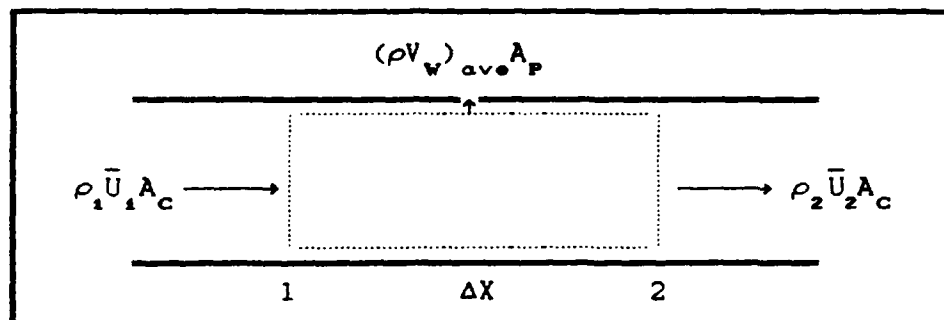


Figure 3-2. Element of Fluid Used For Mass Balance

Performing a mass balance on the fluid element in Figure 3-2

$$\rho_2 \bar{U}_2 A_c = \rho_1 \bar{U}_1 A_c - (\rho V_w)_{ave} A_p \quad (3-7)$$

where  $(\rho V_w)_{ave}$  is the average mass flux through the pipe walls over the increment  $\Delta X$  found by applying Equation (2-2) at stations 1 and 2 (shown in Figure 3-2) and taking the average of the two. The quantity  $(\rho V_w)_{ave}$  is considered negative for blowing, and is considered positive for suction. Equation (3-7) can be solved for  $\bar{U}_2$  giving

$$\bar{U}_2 = \frac{\rho_1 \bar{U}_1}{\rho_2} - \frac{(\rho V_W)_{ave} A_P}{\rho_2 A_C} \quad (3-8)$$

The velocity  $\bar{U}_1$  is taken from the previous step and is initially zero.

The pressure at each step was found by interpolating from the input pressure distribution using the second degree interpolation formula outlined by Holladay (13). The temperature (T), viscosity ( $\mu$ ), axial Reynolds number, and radial Reynolds number were calculated from the following expressions:

$$T = \frac{T_o}{\left[ 1 + \frac{(\gamma - 1)M^2}{2} \right]} ; T = T_o \quad (3-11)$$

$$\mu = \frac{2.27E-08 \cdot (T)^{1.5}}{(T + 198.6)} \quad (3-12)$$

$$Re_x = \frac{4\dot{m}_{ave}}{[\pi D \mu g_c]} = \frac{\rho \bar{U} D}{[\mu g_c]} \quad (3-13)$$

$$Re_w = \frac{(\rho V_W)_{ave} D}{[\mu g_c]} \quad (3-14)$$

where  $\dot{m}_{ave}$  is the average of  $\dot{m}_1$  and  $\dot{m}_2$ .



Because  $\phi$  in the evaporator was known and nearly constant, the total force for the condenser could be determined.

$$F_c = (P_u - P_d)A_c - \sum_{i=u}^{ce} (\tau_w A_p)_i \quad (3-15)$$

where the subscripts  $u$ ,  $d$ , and  $ce$  represent the beginning of the evaporator, the end of the condenser, and the condenser entrance, respectively. By using average condenser values for axial velocity and density, the average friction coefficient for the condenser could be evaluated using

$$\bar{f}_c = \frac{F_c}{\left[ \frac{\rho_c \bar{U}_c^2}{2g_c} \right] A_c} \quad (3-16)$$

The average condenser axial velocity was calculated as half the axial velocity entering the condenser.

#### Solution Method

A marching technique was used to solve for flow properties along the simulated heat pipe. The static pressure data obtained from the experimental work was first read into the computer code. Next, the program prompted for average values of  $\phi$  for the blowing and suction regions. With predefined constants for the pipe geometry and air properties available, and knowing the initial conditions at

$\xi = 0.0$ , the set of governing equations were used to solve for the downstream Mach number, axial Reynolds number, radial Reynolds number, and friction coefficient for each  $\Delta X$  increment along the pipe.

Three subroutines were utilized to 1) interpolate for intermediate pressures, and solve for flow properties for either 2) incompressible, or 3) compressible flow. These subroutines were individually verified using known input and output values. The main program was verified by using the pure mass case (no friction). Using Shapiro's influence coefficients for pure mass addition (14), with constant specific heat and molecular weight

$$\dot{m} = \dot{m}^* \frac{M \sqrt{2(\gamma+1) \left(1 + \frac{\gamma-1}{2} M^2\right)}}{1 + \gamma M^2} \quad (3-17)$$

and

$$P = P^* \frac{\gamma+1}{1 + \gamma M^2} \quad (3-18)$$

and for a constant wall mass flux,  $\dot{m}''$

$$\frac{d\dot{m}}{\dot{m}} = \frac{dx}{x} \quad (3-19)$$

the Mach number as a function of axial location,  $x$ , can be found using

$$x = \frac{x^* M \sqrt{2(\gamma+1) \left(1 + \frac{\gamma-1}{2} M^2\right)}}{1 + \gamma M^2} \quad (3-20)$$

Selecting the Mach number at the end of the evaporator,  $LE$ , determines  $x^*$  and specifies a Mach number for each axial location. The pressure variation is then known using

$$P = \frac{P_o}{1 + \gamma M^2} \quad (3-21)$$

where  $P_o$  is the pressure at the end of the tube. Solving for the constant mass flux,  $\dot{m}''$ , gives

$$\dot{m}'' = \frac{\dot{m}_{LE}}{\pi D x_{LE}} \quad (3-22)$$

where

$$\dot{m}_{LE} = \left[ \frac{PM\pi D^2}{4} \sqrt{\frac{g_c \gamma}{RT}} \right]_{LE} \quad (3-23)$$

The static pressure in the condenser for the pure mass case mirrors the evaporator solution.

For the experimental cases, the numerical code provided two additional checks. First, the force balance over the entire pipe was calculated. When considering the pipe system, the only forces acting on the fluid are the pressures at the ends of the pipe and the total wall shear force.

$$\text{Force Balance} = (P_U - P_D)A_C - \sum_{i=U}^D (\tau_w A_P)_i \quad (3-24)$$

Ideally, the Force Balance should be zero since the drop in pressure between the two ends of the pipe is a result of the wall shear stress. A relative percent error was provided by dividing the Force Balance by the pressure force and multiplying by 100. The final check made was a mass balance over the entire pipe to see if the total mass injected into the pipe equaled the total mass removed from it. A relative percent error was provided by dividing the mass balance by the mass entering the condenser and multiplying by 100.

#### IV. Discussion of Results

As can be seen from Figure 4-1,  $Re_w$  for all four test cases was relatively constant. As the flow rates increased, the axial variation of  $Re_w$  became more obvious. The largest flow rate case had a 0.9 % change in  $Re_w$  between the beginning of the evaporator and the end of the condenser.

Figure 4-2 shows how the pressure varied axially along the walls of the simulated heat pipe for all four  $Re_w$  cases. The data used to create Figure 4-2 can be found in Appendix A. The pressure variation obtained along the pipe was a result of two effects: 1) the friction encountered along the pipe walls, and 2) the rate of change in momentum along the pipe. For flow without friction, the pressure would drop as the flow accelerated in the evaporator and would completely recover as the flow decelerated in the condenser. The total effect of the wall friction force can be seen as a pressure deficit at the end of the pipe. In each of the four  $Re_w$  cases, the flow did not achieve complete pressure recovery. The pressure drop due to friction was found to increase with increased mass flow rate. For the lowest flow rate case, ( $Re_w = 1.8$ ), the pressure in the condenser dropped instead of rising. This occurred, as predicted by Hornbeck, et. al. for suction radial Reynolds numbers less than approximately 2 (8), because the effect of wall shear is greater than that due to the loss of axial momentum flux.

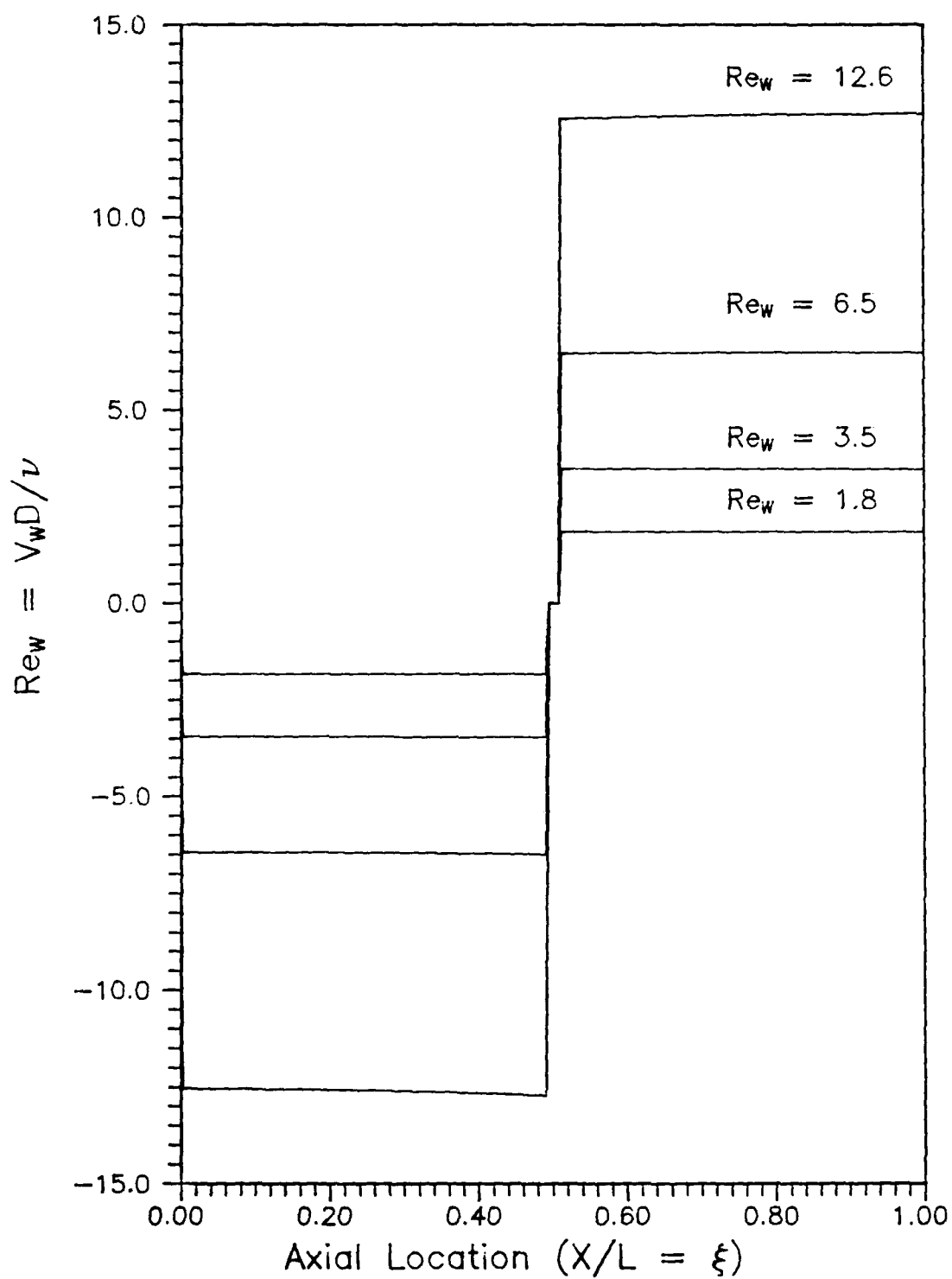


Figure 4-1. Experimental variation of radial Reynolds number with axial location along porous pipe.

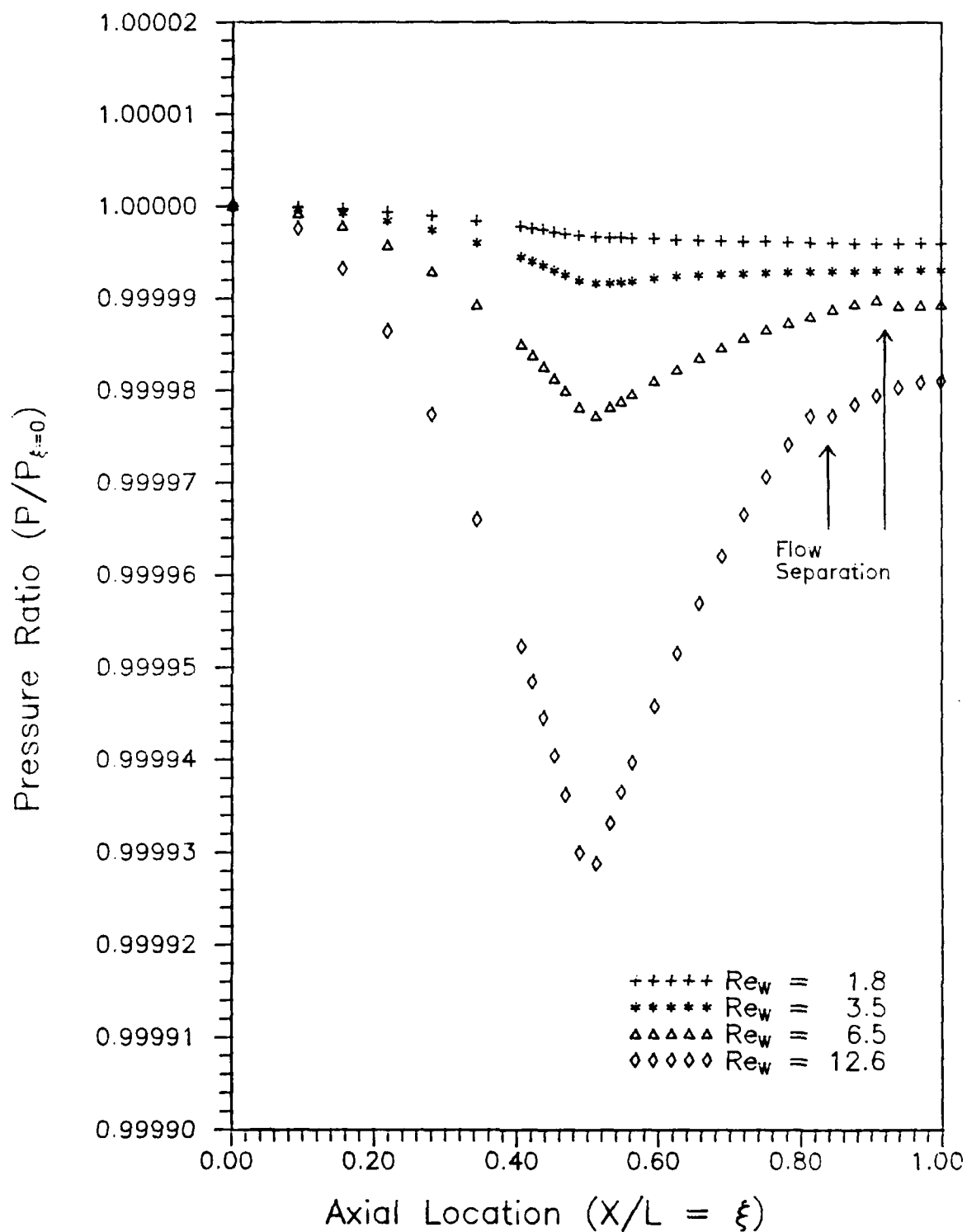


Figure 4-2. Experimental variation of wall static pressure with axial location along porous pipe.

As can be seen in Figure 4-2, flow separation occurred in the condenser for the  $Re_w$  of 6.5 and 12.6 cases. To compare separation locations with those predicted and measured by Quaile and Levy (9), their non-dimensional coordinate system had to be converted to that used in this experiment since they did not have an evaporator region preceding their suction region. Figure 4-3 has three pieces of information: 1) a curve fit of Quaile and Levy's converted theoretical separation predictions, 2) the converted experimental separation locations found by Quaile and Levy, and 3) the separation locations found in this experiment. Recall that Quaile and Levy assumed uniform suction and a parabolic inlet velocity in their derivation of theoretical separation locations. The suction in this experiment was nearly uniform as can be seen in Figure 4-1, however, since the flow entering the suction region was preceded by a blowing region and a short impermeable wall with an  $L/D$  of 1, the velocity profile entering the condenser will be flatter than parabolic, ( $\phi < 1.33$ ). The velocity profile entering the suction region requires some axial distance to adjust to local wall conditions. This would explain why separation in this experiment occurred slightly after that predicted by Quaile and Levy. The two lowest flow rate cases had  $Re_w$ 's less than 4.6, the approximate  $Re_w$  which would cause separation in a fully-developed flow. No flow separation occurred for these



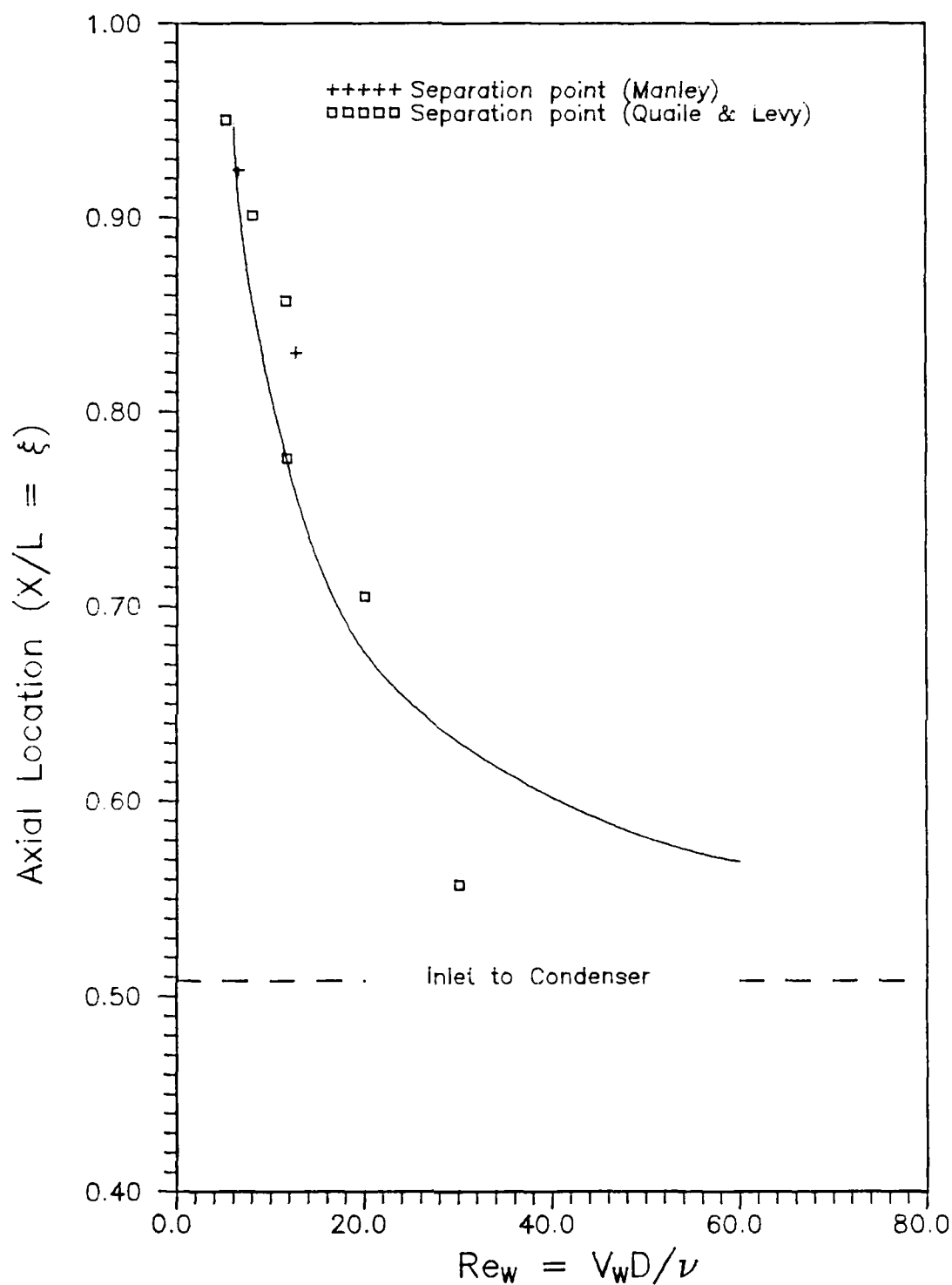


Figure 4-3. Curve Fit of Quaile and Levy's Prediction of Separation for constant wall suction and parabolic inlet velocity profile.

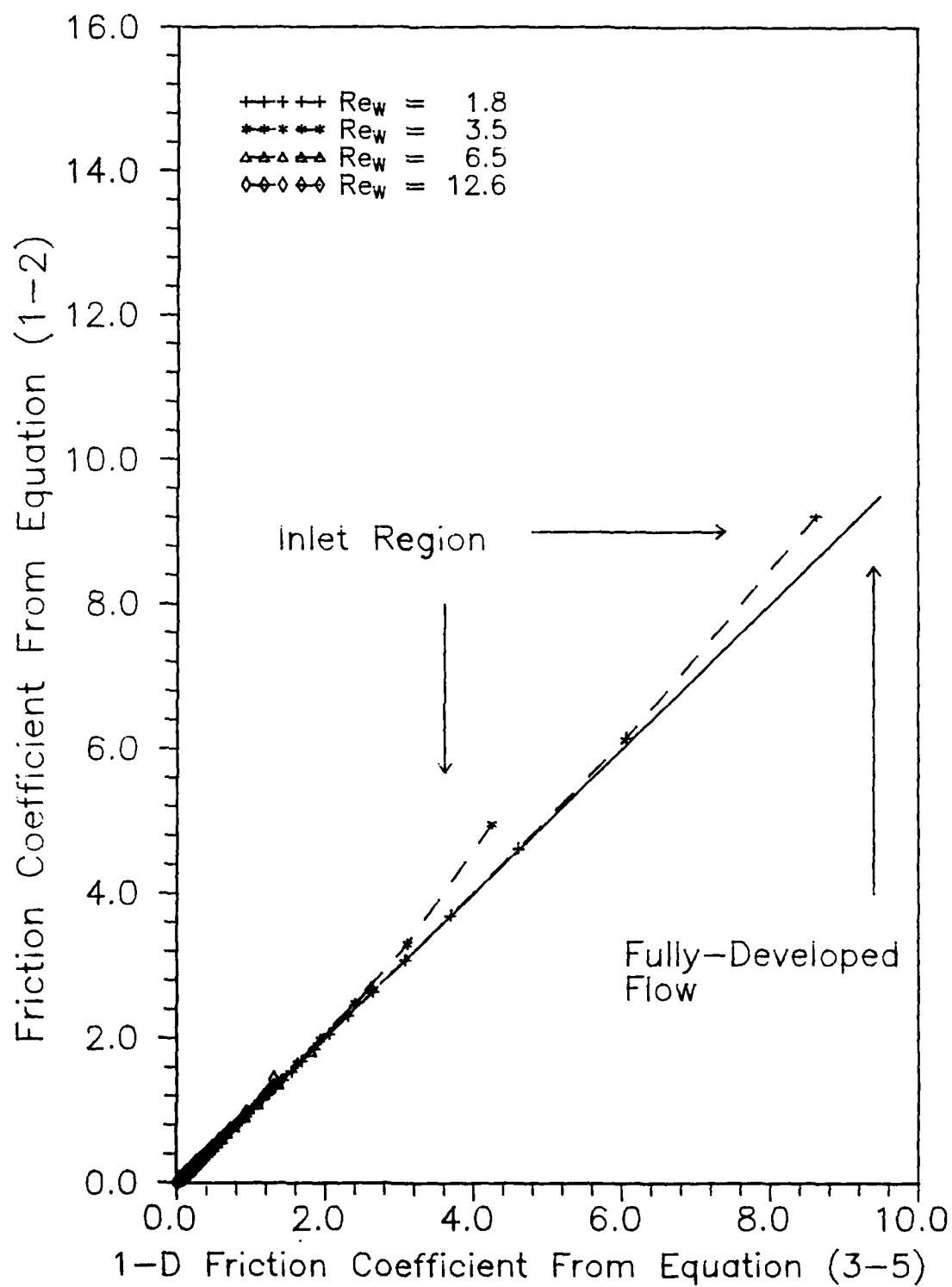


Figure 4-4. Evaporator (Blowing) Friction Coefficient Results.

cases. For the two cases where separation occurred, the axial location plotted in Figure 4-3 corresponds to the center of the two pressure ports detecting separation.

Figure 4-4 is a graph of the evaporator friction coefficients calculated comparing the expression for fully-developed laminar flow, Equation (1-2), with the one-dimensional expression, Equation (3-5). For all four cases, the flow was fully-developed within four  $\Delta X$  increments along the pipe. It should be noted, that the values calculated using Equation (3-5) are highly dependent on  $\phi$ . The values of  $\phi$  used were obtained from a graph Kinney (2) produced numerically assuming fully-developed laminar flow with constant blowing  $Re_w$ 's. Bowman's Equation (1-2) is an empirical curve-fit of Kinney's results. The values obtained from Equation (3-5) differ slightly from those predicted by Kinney. However, by choosing a more appropriate  $\phi$ , Kinney's results can be obtained. The first data points for each  $Re_w$  case plotted correspond to the third increment of the numerical data reduction program. These four data points deviate the farthest from the line for fully-developed laminar flow when compared to respective  $Re_w$  data points

Figure 4-5 is a graph comparing Kinney's (2) theoretical universal law of wall friction for fully-developed laminar flow in porous tubes with uniform suction, with the average condenser friction coefficients,

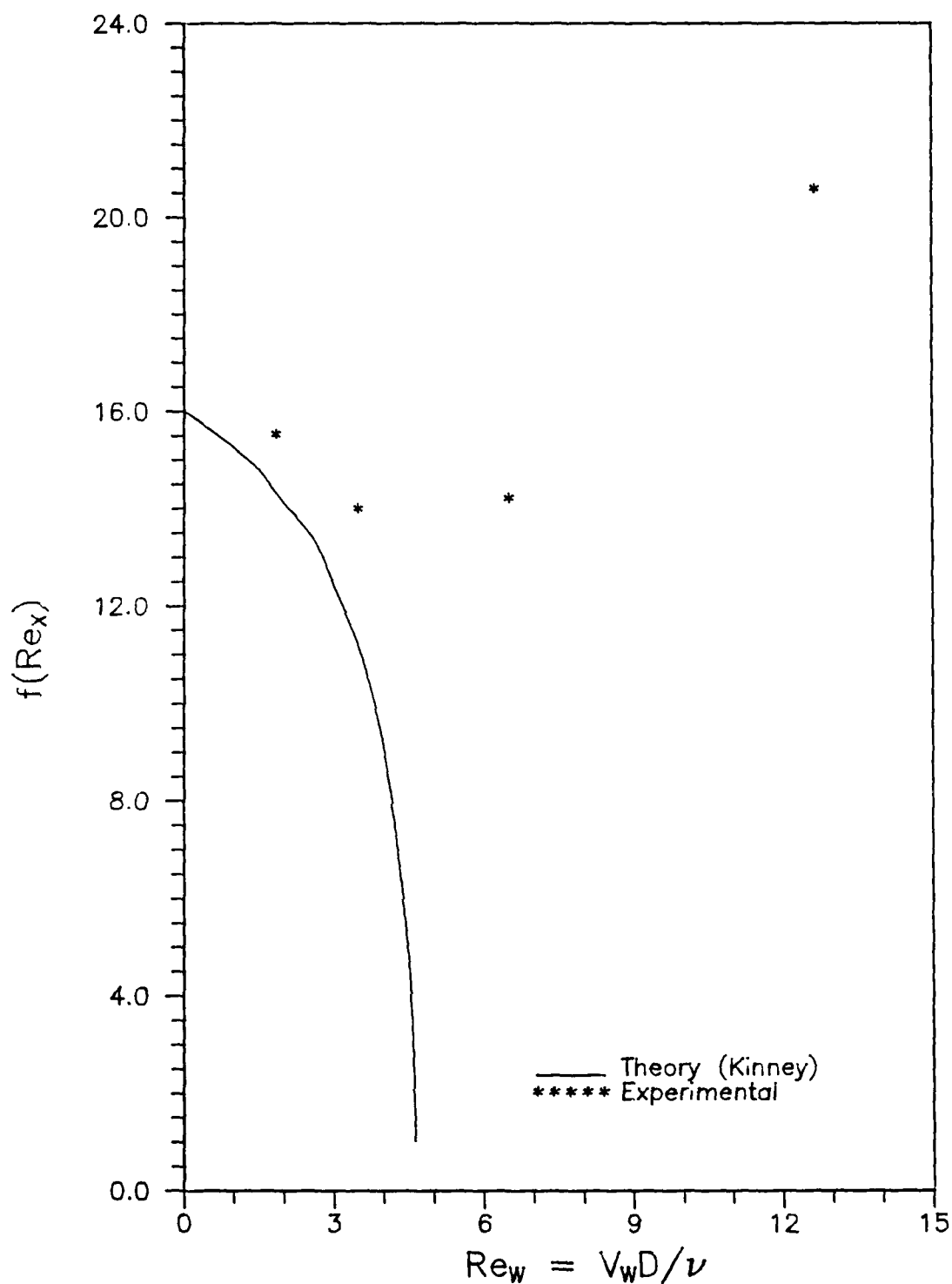


Figure 4-5 Curve fit of Kinney's universal law of wall friction for fully-developed laminar flow in porous tubes and average condenser values from this experiment.

$\bar{f}_c$ , calculated using Equation (3-16). For the two lowest flow rate cases,  $\bar{f}_c$  is slightly higher than that predicted by Kinney. This can be explained by the fact that the flow entering the condenser, due to the blowing in the evaporator, has a flatter velocity profile than the parabolic inlet velocity profile assumed by Kinney. During the length of the condenser where the flow is adjusting to a fully-developed flow, the friction should be higher than the fully-developed values. For the last two flow rate cases, higher friction due to the adjusting velocity profiles, in addition to separated flow would account for the larger deviations from Kinney's theoretical curve. The large friction coefficients after separation would more than balance the small friction coefficients in the regions preceding separation.

Appendix C contains printouts for the four flow rates. These printouts indicate the average values of  $\phi$  used in the blowing and suction regions. They also show the relative percent errors for the force and mass balances encountered during the experimental and numerical data reduction phases. The maximum error was 0.0013 % in the force balance and 0.0312 % in the mass balance.

## V. Conclusions and Recommendations

### Conclusions

The results obtained from this investigation provide insights into the operation of heat pipes at relatively low radial Reynolds numbers. The fully-developed laminar flow solution can be used in the evaporator to obtain friction coefficients. In the condenser, however, the fully-developed solutions may not accurately predict wall friction. Above radial Reynolds numbers of 4.6, the hydrodynamic entrance regions can be a major portion of the condenser length. In heat pipes, unless there exists a sufficiently long adiabatic region, the flow entering the condenser has flatter velocity profiles than those in the impermeable wall case. Through the length of the condenser where the flow is adjusting to local wall conditions, the wall friction will be higher than the fully-developed solution. Also, because of this phenomenon, flow separation will be slightly delayed. In this investigation, an average condenser friction factor was found for radial Reynolds numbers less than 13. This result should prove helpful for design purposes.

### Recommendations

Some ideas for further research are:

- 1) Experimentally determine condenser flow separation locations and average friction coefficients for radial

Reynolds numbers greater than 13, where blowing and suction rates are not constant, and the condenser inlet velocity profile becomes flatter.

2) Determine the onset of transition to turbulent flow and its effect on average condenser friction coefficients.

3) Perform a numerical, two-dimensional flow analysis, using experimental pressure data, to determine appropriate momentum flux factors,  $\phi$ , for the developing flow in the condenser.

### Appendix A: Experimental Data

This appendix contains raw data for the four flow rate cases obtained during the experimental portion of this study. Test run numbers 1, 2, 3, and 4 correspond to radial Reynolds numbers of 3.5, 1.8, 6.5, and 12.6 respectively. All pressures are given in psia and all temperatures are given in °R. The following format is used for all four test cases:

```
test run number
atmospheric pressure
ambient temperature
vacuum tank pressure
port 1 pressure,  $\xi = 0.0$  (beginning of evaporator)
port 2 pressure
port 3 pressure
port 4 pressure
port 5 pressure
port 6 pressure
port 7 pressure
port 8 pressure
port 9 pressure
port 10 pressure
port 11 pressure
port 12 pressure, (last port in evaporator)
port 13 pressure, (first port in condenser)
port 14 pressure
port 15 pressure
port 16 pressure
port 17 pressure
port 18 pressure
port 19 pressure
port 20 pressure
port 21 pressure
port 22 pressure
port 23 pressure
port 24 pressure
port 25 pressure
port 26 pressure
port 27 pressure
port 28 pressure
port 29 pressure
port 30 pressure,  $\xi = 1.0$  (end of condenser)
```



1  
14.282667000000  
526.50  
14.244351480722  
14.263613999968  
14.263609987649  
14.263602540310  
14.263591359022  
14.263576271017  
14.263557421172  
14.263534520094  
14.263528299893  
14.263521720020  
14.263514807101  
14.263507097221  
14.263497110700  
14.263497081109  
14.263498061892  
14.263499050988  
14.263500745013  
14.263504779938  
14.263507824992  
14.263509883195  
14.263511303314  
14.263512510296  
14.263513600389  
14.263514573218  
14.263515434911  
14.263516359503  
14.263517049930  
14.263517850391  
14.263518084766  
14.263518090997  
14.263518091370

2

14.248416000000  
526.00  
14.228081934722  
14.238297320471  
14.238295723592  
14.238292754917  
14.238288259536  
14.238282241124  
14.238274679967  
14.238265590919  
14.238263080953  
14.238260470171  
14.238257765012  
14.238254963998  
14.238251650102  
14.238250005044  
14.238249248215  
14.238248648028  
14.238248065997  
14.238246948099  
14.238245915972  
14.238244968116  
14.238244105078  
14.238243338026  
14.238242661110  
14.238242065994  
14.238241548503  
14.238241108511  
14.238240752108  
14.238240482496  
14.238240294616  
14.238240190500  
14.238240163414

3  
14.302239000000  
526.00  
14.230802744722  
14.266756940340  
14.266746082953  
14.266726010212  
14.266695605500  
14.266654991066  
14.266604022328  
14.266542640400  
14.266525647021  
14.266508007998  
14.266489624021  
14.266470555221  
14.266444511202  
14.266431792928  
14.266445921015  
14.266455020220  
14.266465723482  
14.266485780049  
14.266503172131  
14.266521909861  
14.266537951121  
14.266552664012  
14.266565232023  
14.266576731019  
14.266586102102  
14.266597460074  
14.266605711573  
14.266611421120  
14.266603292385  
14.266604100374  
14.266604363487

4  
14.272881000000  
526.00  
14.133008654431  
14.203597320072  
14.203562960836  
14.203499542432  
14.203403802361  
14.203275260128  
14.203113651026  
14.202918830572  
14.202864878298  
14.202808843901  
14.202750764670  
14.202690523947  
14.202602026204  
14.202584598832  
14.202647510237  
14.202695511205  
14.202740492984  
14.202826570110  
14.202908462280  
14.202985260293  
14.203056868943  
14.203121392452  
14.203178934831  
14.203229592391  
14.203273830120  
14.203274341038  
14.203291310250  
14.203305581193  
14.203318130044  
14.203325605621  
14.203327728798

## Appendix B

10-19-88

Microsoft FORTRAN77 V3.20 02/84

```
D Line# 1      7
1      PROGRAM ONED
2 C     TITLE:  ONE-DIMENSIONAL HEAT PIPE SIMULATION
3 C
4 C     BY:  Captain David Manley
5 C         MS Thesis, 1988
6 C
7 C     This program uses one-dimensional incompressible
      and compressible
8 C     flow models to solve for the flow properties and
      friction
9 C     coefficients in a closed porous pipe with blowing
      and suction.
10 C    The incompressible model is used to calculate the
      flow properties
11 C    until the Mach number reaches 0.01.  Choosing 0.01
      was a purely
12 C    arbitrary decision.  For Mach numbers above 0.01,
      the compressible
13 C    model is used.  The compressible model utilizes
      Shapiro's method
14 C    of influence coefficients to solve for the flow
      properties.
15 C
16 C    *****
17 C    *****  DEFINITION OF VARIABLES  *****
18 C    *****
19 C
20 C    A      Constant obtained from pipe
      calibration used in
21 C            determining wall mass flux
      (lbf/ft/sec)
22 C    AC     Cross-sectional area of the pipe
      (ft2)
23 C    AP     Surface area of DX increment (ft2)
24 C    BETA   Ratio of radial Reynolds number to
25 C            axial Reynolds number
26 C    CL     Condenser Length (ft)
27 C    CC1    Intermediate value used during
      pressure
28 C            interpolation subroutine  (CC2 and
      CC3 are
29 C            similar)
30 C    C2     Speed of sound squared (ft2/sec2)
31 C    D      Pipe inside diameter (ft)
32 C    DMOM   Change in momentum across DX
      increment (lbf)
33 C    DPS    (Pambient)**2 - (P2)**2
      (lbf/ft2)**2
```

34 C	DX	Spacial step size (ft)
35 C	DW	Change in mass flow rate due to mass transfer at the wall (lbm/sec)
36 C		
37 C	DWSUM	Summation of all the incremental mass flow rate changes over the entire pipe due to mass transfer at the wall (lbm/sec)
38 C		
39 C		
40 C	F	Friction factor
41 C	FBARC	Average condenser friction factor
42 C	FBL	Bowman's friction factor for fully-developed laminar flow
43 C		
44 C	FBLREX	Product of FBL and axial Reynolds number
45 C	FBT	Kinney's friction factor for fully-developed turbulent flow
46 C		
47 C	FBTREX	Product of FBT and axial Reynolds number
48 C	FCREXC	Product of FBARC and REXBRC
49 C	FSTAR	No blowing/suction fully-developed turbulent friction coefficient, (Blasius equation)
50 C		
51 C	FUD	Constant to account for the statistical variation of the porous pipe calibration constant A
52 C		
53 C	GAM	Ratio of specific heats
54 C	GC	Newton's gravitational constant (lbm-ft/lbf/sec <sup>2</sup> )
55 C	M1	Mach number at upstream end of DX increment
56 C	M2	Mach number at downstream end of DX increment
57 C	M1S	M1 squared
58 C	M2S	M2 squared
59 C	MFF	Momentum flux factor, (see Kinney pg 1398;IJHMT Vol 11 1968). An indication of the velocity profile or shape
60 C		
61 C		
62 C	MFF1	Momentum flux factor at upstream end of DX increment
63 C		
64 C	MFF2	Momentum flux factor at downstream end of DX increment
65 C		
66 C	MFFB	Blowing momentum flux factor
67 C	MFFS	Suction momentum flux factor

68 C	MSBAR	Average of M1S and M2S
69 C	N	Test Run number
70 C	PATM	Atmospheric pressure (entered in psia then converted to lbf/ft <sup>2</sup> )
71 C		
72 C	PEF	Percent error for force balance
73 C	PEM	Percent error for mass balance
74 C	PF	Pressure force on entire pipe due to the difference of pipe end pressures
75 C		
76 C	PL	Pipe length (ft)
77 C	PND(1)-PND(30)	Non-dimensional static pressure, $P_2/P(X=0.0)$
78 C	P1	Static pressure at upstream end of DX increment (lbf/ft <sup>2</sup> )
79 C		
80 C	P2	Static pressure at downstream end of DX increment (lbf/ft <sup>2</sup> )
81 C		
82 C	P(1)-P(30)	Pressure measurements at corresponding axial positions, X(1)-X(29) (entered in psia and then converted to lbf/ft <sup>2</sup> )
83 C		
84 C		
85 C	R	Ideal gas constant for air (lbf-ft/lbm/R)
86 C	REW	Radial Reynolds number based on pipe inside diameter
87 C		
88 C	REX	Axial Reynolds number based on pipe inside diameter
89 C		
90 C	REXBRC	Average axial Reynolds number for the condenser based on pipe inside diameter. REX entering condenser divided by 2
91 C		
92 C		
93 C	RHOC	Representative density of air for condenser (lbm/ft <sup>3</sup> )
94 C		
95 C	RHO1	Density of air at beginning of DX increment (lbm/ft <sup>3</sup> )
96 C		
97 C	RHO2	Density of air at end of DX increment (lbm/ft <sup>3</sup> )
98 C	RHOV1	Mass flux through the wall at the upstream end of the DX increment (lbm/ft <sup>2</sup> /sec)
99 C		
100 C	RHOV2	Mass flux through the wall at the downstream end of the DX increment (lbm/ft <sup>2</sup> /sec)
101 C		
102 C	RHOVAV	Average mass flux for DX

103 C	RHOBAR	increment (lbm/ft <sup>2</sup> /sec) Average density of air for DX increment (lbm/ft <sup>3</sup> )
104 C	RMU	Viscosity of air (lbf-sec/ft <sup>2</sup> )
105 C	SF	Shear force over the increment DX (lbf)
106 C	SFC	Shear force over the condenser (lbf)
107 C	SFEA	Shear force over the evaporator and adiabatic
108 C		region (lbf)
109 C	SFSUM	Summation of all the incremental shear force
110 C		values over the entire pipe (lbf)
111 C	T	Local static temperature (R)
112 C	TEST	Force balance check (lbf)
113 C	TW	Wall shear stress (lbf/ft <sup>2</sup> )
114 C	TWBARC	Average wall shear stress for the condenser
115 C		(lbf/ft <sup>2</sup> )
116 C	TO	Total air temperature (R)
117 C	UBARC	Average axial velocity in condenser, U entering
118 C		condenser divided by 2 (ft/sec)
119 C	U1	Average velocity at beginning of DX increment
120 C		(ft/sec)
121 C	U2	Average velocity at end of DX increment (ft/sec)
122 C	W1	Mass flow rate at the upstream end of the DX
123 C		increment (lbm/sec)
124 C	W2	Mass flow rate at the downstream end of the DX
125 C		increment (lbm/sec)
126 C	WBAR	Average mass flow rate for DX increment (lbm/sec)
127 C	WCK	Mass flow rate entering condenser (lbm/sec)
128 C	XL	Local axial position (ft)
129 C	XND	Non-dimensional axial position, XL/PL
130 C	XNDD(1)-XNDD(30)	Non-dimensional axial position, X(I)/PL
131 C	X(1)-X(30)	Axial location of pressure measurements (ft)
132 C		
133 C		*****
134 C		* INPUT CONSTANTS AND DECLARE TYPES AND DIMENSIONS *
135 C		*****
136 C		
137	IMPLICIT REAL*8 (A-H,M,O-Z)	



```

138 REAL*8 X(30),P(30),XNDD(30),PND(30)
139 PL = 31.8125/12.0
140 X(1) = 0.0
141 X(2) = 2.90625/12.0
142 X(3) = 4.90625/12.0
143 X(4) = 6.90625/12.0
144 X(5) = 8.90625/12.0
145 X(6) = 10.90625/12.0
146 X(7) = 12.90625/12.0
147 X(8) = 13.40625/12.0
148 X(9) = 13.90625/12.0
149 X(10) = 14.40625/12.0
150 X(11) = 14.90625/12.0
151 X(12) = 15.53125/12.0
152 X(13) = 16.28125/12.0
153 X(14) = 16.90625/12.0
154 X(15) = 17.40625/12.0
155 X(16) = 17.90625/12.0
156 X(17) = 18.90625/12.0
157 X(18) = 19.90625/12.0
158 X(19) = 20.90625/12.0
159 X(20) = 21.90625/12.0
160 X(21) = 22.90625/12.0
161 X(22) = 23.90625/12.0
162 X(23) = 24.90625/12.0
163 X(24) = 25.90625/12.0
164 X(25) = 26.90625/12.0
165 X(26) = 27.90625/12.0
166 X(27) = 28.90625/12.0
167 X(28) = 29.90625/12.0
168 X(29) = 30.90625/12.0
169 X(30) = 31.8125/12.0
170 OPEN (UNIT=9,STATUS='NEW',FILE='C:RESULTS.DAT')
171 OPEN (UNIT=10,STATUS='OLD',FILE='C:DATA.DAT')
172 OPEN (UNIT=11,STATUS='NEW',FILE='C:MACH.DAT')
173 OPEN (UNIT=12,STATUS='NEW',FILE='C:REW.DAT')
174 OPEN (UNIT=13,STATUS='NEW',FILE='C:REX.DAT')
175 OPEN (UNIT=14,STATUS='NEW',FILE='C:P2.DAT')
176 OPEN (UNIT=15,STATUS='NEW',FILE='C:TW.DAT')
177 OPEN (UNIT=16,STATUS='NEW',FILE='C:F.DAT')
178 OPEN (UNIT=17,STATUS='NEW',FILE='C:FBL.DAT')
179 OPEN (UNIT=18,STATUS='NEW',FILE='C:RHOV2.DAT')
180 OPEN (UNIT=19,STATUS='NEW',FILE='C:SF.DAT')
181 OPEN (UNIT=20,STATUS='NEW',FILE='C:DW.DAT')
182 OPEN (UNIT=21,STATUS='NEW',FILE='C:PND.DAT')
183 OPEN (UNIT=22,STATUS='NEW',FILE='C:FREX.DAT')
184 OPEN (UNIT=23,STATUS='NEW',FILE='C:FBLREX.DAT')
185 OPEN (UNIT=24,STATUS='NEW',FILE='C:FBT.DAT')
186 OPEN (UNIT=25,STATUS='NEW',FILE='C:FBTREX.DAT')
187 OPEN (UNIT=26,STATUS='NEW',FILE='C:VERIFY.DAT')
188 OPEN (UNIT=27,STATUS='NEW',FILE='C:FEVAP.DAT')
189 READ (10,4000) N

```

```

190      WRITE (9,5020) N
191      READ (10,4010) PATM
192      WRITE (9,5030) PATM
193      READ (10,4020) T0
194      WRITE (9,5040) T0
195      READ (10,4010) PSINK
196      WRITE (9,5050) PSINK
197      DO 10 I = 1,30
198      READ (10,4010) P(I)
199      P(I) = P(I)*144
200      PND(I) = P(I)/P(1)
201      XNDD(I) = X(I)/PL
202      WRITE (21,5000) XNDD(I),PND(I)
203 10    CONTINUE
204      WRITE (*,5060)
205      READ (*,4030) FUD
206      WRITE (*,5061)
207      READ (*,4030) MFFB
208      WRITE (*,5062)
209      READ (*,4030) MFFS
210      WRITE (9,5070) FUD, MFFB, MFFS
211      PATM = PATM*144
212      PSINK = PSINK*144
213      DX = 0.005
214      A = 3.592472958D8
215      WRITE (9,5080)
216 C
217 C      *****
218 C      * INITIALIZE VARIABLES AT PIPE END, X = 0.0 *
219 C      *****
220 C
221      XL = 0.0
222      W1 = 0.0
223      M1S = 0.0
224      M1 = 0.0
225      U1 = 0.0
226      P1 = P(1)
227      P2 = P1
228      T = T0
229      R = 53.335
230      GC = 32.174
231      PEX = PATM
232      DWSUM = 0.0
233      SFSUM = 0.0
234      I = 1
235      PZ = P(I)
236      PO = P(I+1)
237      PT = P(I+2)
238      XZ = X(I)
239      XO = X(I+1)
240      XT = X(I+2)
241      XND = 0.0

```

```

242      CALL SUBINC
        (FUD,A,T0,PEX,XND,P2,DPS,RHO1,RHOV1,U1,W1,M1,M1S,
243      +DWSUM,T,SFSUM,RHO2,RHOV2,U2,W2,M2S,M2,DW,REX,REW,
        BETA,TW,SF,
244      +F,FBL,FBT,P1,FREX,FBLREX,FBTREX,RHOBAR,UBAR,MFFB,
        MFFS)
245      WRITE (11,5000) XND, M1
246      WRITE (12,5000) XND, REW
247      WRITE (13,5000) XND, M1
248      WRITE (14,5000) XND, P2
249      WRITE (15,5000) XND, M1
250      WRITE (16,5000) XND, M1
251      WRITE (17,5000) XND, M1
252      WRITE (18,5000) XND, RHOV1
253      WRITE (19,5000) XND, M1
254      WRITE (20,5000) XND, DW
255      WRITE (22,5000) XND, M1
256      WRITE (23,5000) XND, M1
257 C
258 C      NOTE: M1 IS USED IN ABOVE WRITE STATEMENTS TO ZERO
        VARIABLES KNOWN
        TO BE ZERO AT END OF PIPE.
259 C
260 C
261      RHOV1 = RHOV2
262      RHO1 = RHO2
263      W1 = W2
264      P1 = P2
265 C
266 C      *****
267 C      ***** BEGIN MARCHING DOWN PIPE *****
268 C      *****
269 C
270      DO 200 J = 1,81
271      K = J
272 C
273 C      *****
274 C      ***** 0.005 < XL < 0.405 *****
275 C      ***** 0.001886 < XND < 0.152770 *****
276 C      *****
277 C
278      XL = XL + DX
279      CALL SUBPRES (PZ,PO,PT,XZ,XO,XT,XL,XND,P2)
280      IF (M1 .LT. 0.01) THEN
281      CALL SUBINC
        (FUD,A,T0,PEX,XND,P2,DPS,RHO1,RHOV1,U1,W1,M1,
282      +M1S,DWSUM,T,SFSUM,RHO2,RHOV2,U2,W2,M2S,M2,DW,REX,REW,
283      +BETA,TW,SF,F,FBL,FBT,P1,FREX,FBLREX,FBTREX,RHOBAR,
284      +UBAR,MFFB,MFFS)
285      ELSE
286      CALL SUBCOMP
        (FUD,A,T0,PEX,XND,P2,DPS,P1,RHO1,RHOV1,U1,W1,
287      +M1,M1S,DWSUM,T,SFSUM,RHO2,RHOV2,U2,W2,M2S,M2,DW,REX

```

```

,REW,
288 +BETA,TW,SF,F,FBL,FBT,FREX,FBLREX,FBTREX,RHOBAR,UBAR)
289 ENDIF
290 WRITE (11,5000) XND,M2
291 WRITE (12,5000) XND,REW
292 WRITE (13,5000) XND,REX
293 WRITE (14,5000) XND,P2
294 WRITE (15,5000) XND,TW
295 WRITE (16,5000) XND,F
296 WRITE (17,5000) XND,FBL
297 WRITE (18,5000) XND,RHOV2
298 WRITE (19,5000) XND,SF
299 WRITE (20,5000) XND,DW
300 WRITE (22,5000) XND,FREX
301 WRITE (23,5000) XND,FBLREX
302 IF (XND.GT. 0.099 .AND. XND.LT. 0.101) THEN
303 WRITE (9,5011) XND,F,REW,REX,BETA,M2,FREX,FBLREX
304 ENDIF
305 C
306 C *****
307 C * CAPTURE OF VARIABLE QUANTITIES TO BE USED TO *
308 C * VERIFIY PROGRAM BY HAND CALCULATION *
309 C *****
310 C
311 IF (K.EQ.3) THEN
312 P1 = P1/144.0
313 P2 = P2/144.0
314 RHOV1 = RHOV1/144.0
315 RHOV2 = RHOV2/144.0
316 RHO1 = RHO1/1728.0
317 RHO2 = RHO2/1728.0
318 RHOBAR = RHOBAR/1728.0
319 U1 = U1*12.0
320 U2 = U2*12.0
321 UBAR = UBAR*12.0
322 DPS = -DPS/20736.0
323 TW = TW/144.0
324 WRITE (26,*) 'K = 3'
325 WRITE (26,*) 'P1 = ',P1
326 WRITE (26,*) 'P2 = ',P2
327 WRITE (26,*) 'RHOV1 = ', RHOV1
328 WRITE (26,*) 'RHOV2 = ', RHOV2
329 WRITE (26,*) 'W1 = ', W1
330 WRITE (26,*) 'W2 = ', W2
331 WRITE (26,*) 'DW = ', DW
332 WRITE (26,*) 'DWSUM = ', DWSUM
333 WRITE (26,*) 'T = ', T
334 WRITE (26,*) 'RHO1 = ', RHO1
335 WRITE (26,*) 'RHO2 = ', RHO2
336 WRITE (26,*) 'RHOBAR = ', RHOBAR
337 WRITE (26,*) 'U1 = ', U1
338 WRITE (26,*) 'U2 = ', U2

```

```

339      WRITE (26,*) 'UBAR = ', UBAR
340      WRITE (26,*) 'M1 = ', M1
341      WRITE (26,*) 'M1S = ', M1S
342      WRITE (26,*) 'M2 = ', M2
343      WRITE (26,*) 'M2S = ', M2S
344      WRITE (26,*) 'ADPS = ', DPS
345      WRITE (26,*) 'F = ', F
346      WRITE (26,*) 'FREX = ', FREX
347      WRITE (26,*) 'TW = ', TW
348      WRITE (26,*) 'SFSUM = ', SFSUM
349      WRITE (26,*) 'SF = ', SF
350      WRITE (26,*) 'REW = ', REW
351      WRITE (26,*) 'REX = ', REX
352      P1 = P1*144.0
353      P2 = P2*144.0
354      RHOV1 = RHOV1*144.0
355      RHOV2 = RHOV2*144.0
356      RHO1 = RHO1*1728.0
357      RHO2 = RHO2*1728.0
358      RHOBAR = RHOBAR*1728.0
359      U1 = U1/12.0
360      U2 = U2/12.0
361      UBAR = UBAR/12.0
362      DPS = -DPS*20736.0
363      TW = TW*144.0
364  ENDIF
365  IF (K.EQ.4) THEN
366      P1 = P1/144.0
367      P2 = P2/144.0
368      RHOV1 = RHOV1/144.0
369      RHOV2 = RHOV2/144.0
370      RHO1 = RHO1/1728.0
371      RHO2 = RHO2/1728.0
372      RHOBAR = RHOBAR/1728.0
373      U1 = U1*12.0
374      U2 = U2*12.0
375      UBAR = UBAR*12.0
376      DPS = -DPS/20736.0
377      TW = TW/144.0
378      WRITE (26,*) ' '
379      WRITE (26,*) 'K = 4'
380      WRITE (26,*) 'P1 = ', P1
381      WRITE (26,*) 'P2 = ', P2
382      WRITE (26,*) 'RHOV1 = ', RHOV1
383      WRITE (26,*) 'RHOV2 = ', RHOV2
384      WRITE (26,*) 'W1 = ', W1
385      WRITE (26,*) 'W2 = ', W2
386      WRITE (26,*) 'DW = ', DW
387      WRITE (26,*) 'DWSUM = ', DWSUM
388      WRITE (26,*) 'T = ', T
389      WRITE (26,*) 'RHO1 = ', RHO1
390      WRITE (26,*) 'RHO2 = ', RHO2

```

```

391      WRITE (26,*) 'RHOBAR = ', RHOBAR
392      WRITE (26,*) 'U1 = ', U1
393      WRITE (26,*) 'U2 = ', U2
394      WRITE (26,*) 'UBAR = ', UBAR
395      WRITE (26,*) 'M1 = ', M1
396      WRITE (26,*) 'M1S = ', M1S
397      WRITE (26,*) 'M2 = ', M2
398      WRITE (26,*) 'M2S = ', M2S
399      WRITE (26,*) 'ADPS = ', DPS
400      WRITE (26,*) 'F = ', F
401      WRITE (26,*) 'FREX = ', FREX
402      WRITE (26,*) 'TW = ', TW
403      WRITE (26,*) 'SFSUM = ', SFSUM
404      WRITE (26,*) 'SF = ', SF
405      WRITE (26,*) 'REW = ', REW
406      WRITE (26,*) 'REX = ', REX
407      P1 = P1*144.0
408      P2 = P2*144.0
409      RHOV1 = RHOV1*144.0
410      RHOV2 = RHOV2*144.0
411      RHO1 = RHO1*1728.0
412      RHO2 = RHO2*1728.0
413      RHOBAR = RHOBAR*1728.0
414      U1 = U1/12.0
415      U2 = U2/12.0
416      UBAR = UBAR/12.0
417      DPS = -DPS*20736.0
418      TW = TW*144.0
419      ENDIF
420 C
421 C *****
422 C ***** END OF VERIFICATION ROUTINE *****
423 C *****
424 C
425      RHOV1 = RHOV2
426      RHO1 = RHO2
427      W1 = W2
428      M1S = M2S
429      M1 = M2
430      U1 = U2
431      P1 = P2
432 200 CONTINUE
433      I = 3
434      PZ = P(I)
435      PO = P(I+1)
436      PT = P(I+2)
437      XZ = X(I)
438      XO = X(I+1)
439      XT = X(I+2)
440      DO 400 J = 1,67
441 C

```

```

442 C *****
443 C ***** 0.410 < XL < 0.740 *****
444 C ***** 0.154656 < XND < 0.279136 *****
445 C *****
446 C
447 XL = XL + DX
448 CALL SUBPRES (PZ,PO,PT,XZ,XO,XT,XL,XND,P2)
449 IF (M1 .LT. 0.01) THEN
450 CALL SUBINC
    (FUD,A,T0,PEX,XND,P2,DPS,RHO1,RHOV1,U1,W1,M1,
451 +M1S,DWSUM,T,SFSUM,RHO2,RHOV2,U2,W2,M2S,M2,DW,REX,REW,
452 +BETA,TW,SF,F,FBL,FBT,P1,FREX,FBLREX,FBTREX,RHOBAR,
453 +UBAR,MFFB,MFFS)
454 ELSE
455 CALL SUBCOMP
    (FUD,A,T0,PEX,XND,P2,DPS,P1,RHO1,RHOV1,U1,W1,
456 +M1,M1S,DWSUM,T,SFSUM,RHO2,RHOV2,U2,W2,M2S,M2,DW,REX
    ,REW,
457 +BETA,TW,SF,F,FBL,FBT,FREX,FBLREX,FBTREX,RHOBAR,UBAR)
458 ENDIF
459 WRITE (11,5000) XND,M2
460 WRITE (12,5000) XND,REW
461 WRITE (13,5000) XND,REX
462 WRITE (14,5000) XND,P2
463 WRITE (15,5000) XND,TW
464 WRITE (16,5000) XND,F
465 WRITE (17,5000) XND,FBL
466 WRITE (18,5000) XND,RHOV2
467 WRITE (19,5000) XND,SF
468 WRITE (20,5000) XND,DW
469 WRITE (22,5000) XND,FREX
470 WRITE (23,5000) XND,FBLREX
471 IF (XND .GT. 0.199 .AND. XND .LT. 0.201) THEN
472 WRITE (9,5011) XND,F,REW,REX,BETA,M2,FREX,FBLREX
473 ENDIF
474 RHOV1 = RHOV2
475 RHO1 = RHO2
476 W1 = W2
477 M1S = M2S
478 M1 = M2
479 U1 = U2
480 P1 = P2
481 400 CONTINUE
482 I = 5
483 PZ = P(I)
484 PO = P(I+1)
485 PT = P(I+2)
486 XZ = X(I)
487 XO = X(I+1)
488 XT = X(I+2)
489 DO 600 J = 1,67
490 C

```

```

491 C      *****
492 C      ***** 0.745 < XL < 1.075 *****
493 C      ***** 0.281022 < XND < 0.405501 *****
494 C      *****
495 C
496      XL = XL + DX
497      CALL SUBPRES (PZ,PO,PT,XZ,XO,XT,XL,XND,P2)
498      IF (M1 .LT. 0.01) THEN
499      CALL SUBINC
      (FUD,A,T0,PEX,XND,P2,DPS,RHO1,RHOV1,U1,W1,M1,
500      +M1S,DWSUM,T,SFSUM,RHO2,RHOV2,U2,W2,M2S,M2,DW,REX,REW,
501      +BETA,TW,SF,F,FBL,FBT,P1,FREX,FBLREX,FBTREX,RHOBAR,
502      +UBAR,MFFB,MFFS)
503      ELSE
504      CALL SUBCOMP
      (FUD,A,T0,PEX,XND,P2,DPS,P1,RHO1,RHOV1,U1,W1,
505      +M1,M1S,DWSUM,T,SFSUM,RHO2,RHOV2,U2,W2,M2S,M2,DW,REX
      ,REW,
506      +BETA,TW,SF,F,FBL,FBT,FREX,FBLREX,FBTREX,RHOBAR,UBAR)
507      ENDIF
508      WRITE (11,5000) XND,M2
509      WRITE (12,5000) XND,REW
510      WRITE (13,5000) XND,REX
511      WRITE (14,5000) XND,P2
512      WRITE (15,5000) XND,TW
513      WRITE (16,5000) XND,F
514      WRITE (17,5000) XND,FBL
515      WRITE (18,5000) XND,RHOV2
516      WRITE (19,5000) XND,SF
517      WRITE (20,5000) XND,DW
518      WRITE (22,5000) XND,FREX
519      WRITE (23,5000) XND,FBLREX
520      IF (XND .GT. 0.298 .AND. XND .LT. 0.301) THEN
521      WRITE (9,5011) XND,F,REW,REX,BETA,M2,FREX,FBLREX
522      ENDIF
523      IF (XND .GT. 0.398 .AND. XND .LT. 0.401) THEN
524      WRITE (9,5011) XND,F,REW,REX,BETA,M2,FREX,FBLREX
525      ENDIF
526      RHOV1 = RHOV2
527      RHO1 = RHO2
528      W1 = W2
529      M1S = M2S
530      M1 = M2
531      U1 = U2
532      P1 = P2
533 600    CONTINUE
534      I = 7
535      PZ = P(I)
536      PO = P(I+1)
537      PT = P(I+2)
538      XZ = X(I)
539      XO = X(I+1)

```



```

540      XT = X(I+2)
541      DO 800 J = 1,16
542 C
543 C      *****
544 C      ***** 1.080 < XL < 1.155 *****
545 C      ***** 0.407387 < XND < 0.435678 *****
546 C      *****
547 C
548      XL = XL + DX
549      CALL SUBPRES (PZ,PO,PT,XZ,XO,XT,XL,XND,P2)
550      IF (M1 .LT. 0.01) THEN
551      CALL SUBINC
552      (FUD,A,TO,PEX,XND,P2,DPS,RHO1,RHOV1,U1,W1,M1,
553      +M1S,DWSUM,T,SFSUM,RHO2,RHOV2,U2,W2,M2S,M2,DW,REX,REW,
554      +BETA,TW,SF,F,FBL,FBT,P1,FREX,FBLREX,FBTREX,RHOBAR,
555      +UBAR,MFFB,MFFS)
556      ELSE
557      CALL SUBCOMP
558      (FUD,A,TO,PEX,XND,P2,DPS,P1,RHO1,RHOV1,U1,W1,
559      +M1,M1S,DWSUM,T,SFSUM,RHO2,RHOV2,U2,W2,M2S,M2,DW,REX,
560      +REW,
561      +BETA,TW,SF,F,FBL,FBT,FREX,FBLREX,FBTREX,RHOBAR,UBAR)
562      ENDIF
563      WRITE (11,5000) XND,M2
564      WRITE (12,5000) XND,REW
565      WRITE (13,5000) XND,REX
566      WRITE (14,5000) XND,P2
567      WRITE (15,5000) XND,TW
568      WRITE (16,5000) XND,F
569      WRITE (17,5000) XND,FBL
570      WRITE (18,5000) XND,RHOV2
571      WRITE (19,5000) XND,SF
572      WRITE (20,5000) XND,DW
573      WRITE (22,5000) XND,FREX
574      WRITE (23,5000) XND,FBLREX
575      RHOV1 = RHOV2
576      RHO1 = RHO2
577      W1 = W2
578      M1S = M2S
579      M1 = M2
580      U1 = U2
581      P1 = P2
582      CONTINUE
583      I = 9
584      PZ = P(I)
585      PO = P(I+1)
586      PT = P(I+2)
587      XZ = X(I)
588      XO = X(I+1)
589      XT = X(I+2)
590      DO 1000 J = 1,17
591 C

```

```

589 C *****
590 C ***** 1.160 < XL < 1.240 *****
591 C ***** 0.437564 < XND < 0.467741 *****
592 C *****
593 C
594 XL = XL + DX
595 CALL SUBPRES (PZ,PO,PT,XZ,XO,XT,XL,XND,P2)
596 IF (M1 .LT. 0.01) THEN
597 CALL SUBINC
    (FUD,A,T0,PEX,XND,P2,DPS,RHO1,RHOV1,U1,W1,M1,
598 +M1S,DWSUM,T,SFSUM,RHO2,RHOV2,U2,W2,M2S,M2,DW,REX,REW,
599 +BETA,TW,SF,F,FBL,FBT,P1,FREX,FBLREX,FBTREX,RHOBAR,
600 +UBAR,MFFB,MFFS)
601 ELSE
602 CALL SUBCOMP
    (FUD,A,T0,PEX,XND,P2,DPS,P1,RHO1,RHOV1,U1,W1,
603 +M1,M1S,DWSUM,T,SFSUM,RHO2,RHOV2,U2,W2,M2S,M2,DW,REX
    ,REW,
604 +BETA,TW,SF,F,FBL,FBT,FREX,FBLREX,FBTREX,RHOBAR,UBAR)
605 ENDIF
606 WRITE (11,5000) XND,M2
607 WRITE (12,5000) XND,REW
608 WRITE (13,5000) XND,REX
609 WRITE (14,5000) XND,P2
610 WRITE (15,5000) XND,TW
611 WRITE (16,5000) XND,F
612 WRITE (17,5000) XND,FBL
613 WRITE (18,5000) XND,RHOV2
614 WRITE (19,5000) XND,SF
615 WRITE (20,5000) XND,DW
616 WRITE (22,5000) XND,FREX
617 WRITE (23,5000) XND,FBLREX
618 RHOV1 = RHOV2
619 RHO1 = RHO2
620 W1 = W2
621 M1S = M2S
622 M1 = M2
623 U1 = U2
624 P1 = P2
625 1000 CONTINUE
626 I = 11
627 PZ = P(I)
628 PO = P(I+1)
629 PT = P(I+2)
630 XZ = X(I)
631 XO = X(I+1)
632 XT = X(I+2)
633 DO 1200 J = 1,23
634 C
635 C *****
636 C ***** 1.245 < XL < 1.355 *****
637 C ***** 0.469627 < XND < 0.511120 *****

```

```

638 C      *****
639 C
640      XL = XL + DX
641      CALL SUBPRES (PZ,PO,PT,XZ,XO,XT,XL,XND,P2)
642      IF (XND .GT. 0.491 .AND. XND .LT. 0.508) PEX = P2
643      IF (XND .GT. 0.508) PEX = PSINK
644      IF (M1 .LT. 0.01) THEN
645      CALL SUBINC
        (FUD,A,TO,PEX,XND,P2,DPS,RHO1,RHOV1,U1,W1,M1,
646      +M1S,DWSUM,T,SFSUM,RHO2,RHOV2,U2,W2,M2S,M2,DW,REX,REW,
647      +BETA,TW,SF,F,FBL,FBT,P1,FREX,FBLREX,FBTREX,RHOBAR,
648      +UBAR,MFFB,MFFS)
649      ELSE
650      CALL SUBCOMP
        (FUD,A,TO,PEX,XND,P2,DPS,P1,RHO1,RHOV1,U1,W1,
651      +M1,M1S,DWSUM,T,SFSUM,RHO2,RHOV2,U2,W2,M2S,M2,DW,REX
        ,REW,
652      +BETA,TW,SF,F,FBL,FBT,FREX,FBLREX,FBTREX,RHOBAR,UBAR)
653      ENDIF
654      WRITE (11,5000) XND,M2
655      WRITE (12,5000) XND,REW
656      WRITE (13,5000) XND,REX
657      WRITE (14,5000) XND,P2
658      WRITE (15,5000) XND,TW
659      WRITE (16,5000) XND,F
660      WRITE (17,5000) XND,FBL
661      WRITE (18,5000) XND,RHOV2
662      WRITE (19,5000) XND,SF
663      WRITE (20,5000) XND,DW
664      WRITE (22,5000) XND,FREX
665      WRITE (23,5000) XND,FBLREX
666      IF (XND .GT. 0.508) THEN
667      WRITE (24,5000) XND,FBT
668      WRITE (25,5000) XND,FBTREX
669      ENDIF
670      IF (XND .GT. 0.506 .AND. XND .LT. 0.508) THEN
671      UBARC = UBAR/2
672      REXBRC = REX/2
673      ENDIF
674      IF (XND .GT. 0.508 .AND. XND .LT. 0.510) THEN
675      SFEA = SFSUM
676      RHOC = RHO2
677      ENDIF
678      RHOV1 = RHOV2
679      RHO1 = RHO2
680      W1 = W2
681      M1S = M2S
682      M1 = M2
683      U1 = U2
684      P1 = P2
685      IF (XND .GT. 0.489 .AND. XND .LT. 0.491) WCK = DWSUM
686 1200 CONTINUE

```

```

687      I = 13
688      PZ = P(I)
689      PO = P(I+1)
690      PT = P(I+2)
691      XZ = X(I)
692      XO = X(I+1)
693      XT = X(I+2)
694      DO 1400 J = 1,19
695 C
696 C      *****
697 C      ***** 1.360 < XL < 1.450 *****
698 C      ***** 0.513006 < XND < 0.546955 *****
699 C      *****
700 C
701      XL = XL + DX
702      CALL SUBPRES (PZ,PO,PT,XZ,XO,XT,XL,XND,P2)
703      IF (M1 .LT. 0.01) THEN
704      CALL SUBINC
        (FUD,A,T0,PEX,XND,P2,DPS,RHO1,RHOV1,U1,W1,M1,
705      +M1S,DWSUM,T,SFSUM,RHO2,RHOV2,U2,W2,M2S,M2,DW,REX,REW,
706      +BETA,TW,SF,F,FBL,FBT,P1,FREX,FBLREX,FBTREX,RHOBAR,
707      +UBAR,MFFB,MFFS)
708      ELSE
709      CALL SUBCOMP
        (FUD,A,T0,PEX,XND,P2,DPS,P1,RHO1,RHOV1,U1,W1,
710      +M1,M1S,DWSUM,T,SFSUM,RHO2,RHOV2,U2,W2,M2S,M2,DW,REX
        ,REW,
711      +BETA,TW,SF,F,FBL,FBT,FREX,FBLREX,FBTREX,RHOBAR,UBAR)
712      ENDIF
713      WRITE (11,5000) XND,M2
714      WRITE (12,5000) XND,REW
715      WRITE (13,5000) XND,REX
716      WRITE (14,5000) XND,P2
717      WRITE (15,5000) XND,TW
718      WRITE (16,5000) XND,F
719      WRITE (17,5000) XND,FBL
720      WRITE (18,5000) XND,RHOV2
721      WRITE (19,5000) XND,SF
722      WRITE (20,5000) XND,DW
723      WRITE (22,5000) XND,FREX
724      WRITE (23,5000) XND,FBLREX
725      WRITE (24,5000) XND,FBT
726      WRITE (25,5000) XND,FBTREX
727      RHOV1 = RHOV2
728      RHO1 = RHO2
729      W1 = W2
730      M1S = M2S
731      M1 = M2
732      U1 = U2
733      P1 = P2
734 1400 CONTINUE
735      I = 15

```

```

736      PZ = P(I)
737      PO = P(I+1)
738      PT = P(I+2)
739      XZ = X(I)
740      XO = X(I+1)
741      XT = X(I+2)
742      DO 1600 J = 1,25
743 C
744 C      *****
745 C      ***** 1.455 < XL < 1.575 *****
746 C      ***** 0.548841 < XND < 0.594106 *****
747 C      *****
748 C
749      XL = XL + DX
750      CALL SUBPRES (PZ,PO,PT,XZ,XO,XT,XL,XND,P2)
751      IF (M1 .LT. 0.01) THEN
752      CALL SUBINC
       (FUD,A,T0,PEX,XND,P2,DPS,RHO1,RHOV1,U1,W1,M1,
753      +M1S,DWSUM,T,SFSUM,RHO2,RHOV2,U2,W2,M2S,M2,DW,REX,REW,
754      +BETA,TW,SF,F,FBL,FBT,P1,FREX,FBLREX,FBTREX,RHOBAR,
755      +UBAR,MFFB,MFFS)
756      ELSE
757      CALL SUBCOMP
       (FUD,A,T0,PEX,XND,P2,DPS,P1,RHO1,RHOV1,U1,W1,
758      +M1,M1S,DWSUM,T,SFSUM,RHO2,RHOV2,U2,W2,M2S,M2,DW,REX
       ,REW,
759      +BETA,TW,SF,F,FBL,FBT,FREX,FBLREX,FBTREX,RHOBAR,UBAR)
760      ENDIF
761      WRITE (11,5000) XND,M2
762      WRITE (12,5000) XND,REW
763      WRITE (13,5000) XND,REX
764      WRITE (14,5000) XND,P2
765      WRITE (15,5000) XND,TW
766      WRITE (16,5000) XND,F
767      WRITE (17,5000) XND,FBL
768      WRITE (18,5000) XND,RHOV2
769      WRITE (19,5000) XND,SF
770      WRITE (20,5000) XND,DW
771      WRITE (22,5000) XND,FREX
772      WRITE (23,5000) XND,FBLREX
773      WRITE (24,5000) XND,FBT
774      WRITE (25,5000) XND,FBTREX
775      RHOV1 = RHOV2
776      RHO1 = RHO2
777      W1 = W2
778      M1S = M2S
779      M1 = M2
780      U1 = U2
781      P1 = P2
782 1600  CONTINUE
783      I = I + 1
784      PZ = P(I)

```

```

785      PO = P(I+1)
786      PT = P(I+2)
787      XZ = X(I)
788      XO = X(I+1)
789      XT = X(I+2)
790      DO 1800 J = 1,33
791 C
792 C      *****
793 C      ***** 1.580 < XL < 1.740 *****
794 C      ***** 0.595992 < XND < 0.656346 *****
795 C      *****
796 C
797      XL = XL + DX
798      CALL SUBPRES (PZ,PO,PT,XZ,XO,XT,XL,XND,P2)
799      IF (M1 .LT. 0.01) THEN
800      CALL SUBINC
      (FUD,A,T0,PEX,XND,P2,DPS,RHO1,RHOV1,U1,W1,M1,
801      +M1S,DWSUM,T,SFSUM,RHO2,RHOV2,U2,W2,M2S,M2,DW,REW,
802      +BETA,TW,SF,F,FBL,FBT,P1,FREX,FBLREX,FBTREX,RHOBAR,
803      +UBAR,MFFB,MFFS)
804      ELSE
805      CALL SUBCOMP
      (FUD,A,T0,PEX,XND,P2,DPS,P1,RHO1,RHOV1,U1,W1,
806      +M1,M1S,DWSUM,T,SFSUM,RHO2,RHOV2,U2,W2,M2S,M2,DW,REW,
      +BETA,TW,SF,F,FBL,FBT,FREX,FBLREX,FBTREX,RHOBAR,UBAR)
807      ENDIF
808      WRITE (11,5000) XND,M2
809      WRITE (12,5000) XND,REW
810      WRITE (13,5000) XND,REW
811      WRITE (14,5000) XND,P2
812      WRITE (15,5000) XND,TW
813      WRITE (16,5000) XND,F
814      WRITE (17,5000) XND,FBL
815      WRITE (18,5000) XND,RHOV2
816      WRITE (19,5000) XND,SF
817      WRITE (20,5000) XND,DW
818      WRITE (22,5000) XND,FREX
819      WRITE (23,5000) XND,FBLREX
820      WRITE (24,5000) XND,FBT
821      WRITE (25,5000) XND,FBTREX
822      IF (XND .GT. 0.599 .AND. XND .LT. 0.601) THEN
823      WRITE (9,5010)
      XND,F,REW,REW,REX,BETA,M2,FREX,FBLREX,FBTREX
824      ENDIF
825      ENDIF
826      RHOV1 = RHOV2
827      RHO1 = RHO2
828      W1 = W2
829      M1S = M2S
830      M1 = M2
831      U1 = U2
832      P1 = P2

```

```

833 1800 CONTINUE
834      I = 19
835      PZ = P(I)
836      PO = P(I+1)
837      PT = P(I+2)
838      XZ = X(I)
839      XO = X(I+1)
840      XT = X(I+2)
841      DO 2000 J = 1,33
842 C
843 C      *****
844 C      ***** 1.745 < XL < 1.905 *****
845 C      ***** 0.658232 < XND < 0.718585 *****
846 C      *****
847 C
848      XL = XL + DX
849      CALL SUBPRES (PZ,PO,PT,XZ,XO,XT,XL,XND,P2)
850      IF (M1 .LT. 0.01) THEN
851      CALL SUBINC
      (FUD,A,T0,PEX,XND,P2,DPS,RHO1,RHOV1,U1,W1,M1,
852 +M1S,DWSUM,T,SFSUM,RHO2,RHOV2,U2,W2,M2S,M2,DW,REX,REW,
853 +BETA,TW,SF,F,FBL,FBT,P1,FREX,FBLREX,FBTREX,RHOBAR,
854 +UBAR,MFFB,MFFS)
855      ELSE
856      CALL SUBCOMP
      (FUD,A,T0,PEX,XND,P2,DPS,P1,RHO1,RHOV1,U1,W1,
857 +M1,M1S,DWSUM,T,SFSUM,RHO2,RHOV2,U2,W2,M2S,M2,DW,REX,
      REW,
858 +BETA,TW,SF,F,FBL,FBT,FREX,FBLREX,FBTREX,RHOBAR,UBAR)
859      ENDIF
860      WRITE (11,5000) XND,M2
861      WRITE (12,5000) XND,REW
862      WRITE (13,5000) XND,REX
863      WRITE (14,5000) XND,P2
864      WRITE (15,5000) XND,TW
865      WRITE (16,5000) XND,F
866      WRITE (17,5000) XND,FBL
867      WRITE (18,5000) XND,RHOV2
868      WRITE (19,5000) XND,SF
869      WRITE (20,5000) XND,DW
870      WRITE (22,5000) XND,FREX
871      WRITE (23,5000) XND,FBLREX
872      WRITE (24,5000) XND,FBT
873      WRITE (25,5000) XND,FBTREX
874      IF (XND .GT. 0.698 .AND. XND .LT. 0.701) THEN
875      WRITE (9,5010)
      XND,F,REW,REX,BETA,M2,FREX,FBLREX,FBTREX
876      ENDIF
877      RHOV1 = RHOV2
878      RHO1 = RHO2
879      W1 = W2
880      M1S = M2S

```

```

881      M1 = M2
882      U1 = U2
883      P1 = P2
884 2000  CONTINUE
885      I = 21
886      PZ = P(I)
887      PO = P(I+1)
888      PT = P(I+2)
889      XZ = X(I)
890      XO = X(I+1)
891      XT = X(I+2)
892      DO 2200 J = 1,34
893 C
894 C      *****
895 C      ***** 1.910 < XL < 2.075 *****
896 C      ***** 0.720472 < XND < 0.782711 *****
897 C      *****
898 C
899      XL = XL + DX
900      CALL SUBPRES (PZ,PO,PT,XZ,XO,XT,XL,XND,P2)
901      IF (M1 .LT. 0.01) THEN
902      CALL SUBINC
903      (FUD,A,T0,PEX,XND,P2,DPS,RHO1,RHOV1,U1,W1,M1,
904      +M1S,DWSUM,T,SFSUM,RHO2,RHOV2,U2,W2,M2S,M2,DW,REX,REW,
905      +BETA,TW,SF,F,FBL,FBT,P1,FREX,FBLREX,FBTREX,RHOBAR,
906      +UBAR,MFFB,MFFS)
907      ELSE
908      CALL SUBCOMP
909      (FUD,A,T0,PEX,XND,P2,DPS,P1,RHO1,RHOV1,U1,W1,
910      +M1,M1S,DWSUM,T,SFSUM,RHO2,RHOV2,U2,W2,M2S,M2,DW,REX
911      ,REW,
912      +BETA,TW,SF,F,FBL,FBT,FREX,FBLREX,FBTREX,RHOBAR,UBAR)
913      ENDIF
914      WRITE (11,5000) XND,M2
915      WRITE (12,5000) XND,REW
916      WRITE (13,5000) XND,REX
917      WRITE (14,5000) XND,P2
918      WRITE (15,5000) XND,TW
919      WRITE (16,5000) XND,F
920      WRITE (17,5000) XND,FBL
921      WRITE (18,5000) XND,RHOV2
922      WRITE (19,5000) XND,SF
923      WRITE (20,5000) XND,DW
924      WRITE (22,5000) XND,FREX
925      WRITE (23,5000) XND,FBLREX
926      WRITE (24,5000) XND,FBT
927      WRITE (25,5000) XND,FBTREX
928      RHOV1 = RHOV2
929      RHO1 = RHO2
930      W1 = W2
931      M1S = M2S
932      M1 = M2

```



```

930      U1 = U2
931      P1 = P2
932 2200  CONTINUE
933      I = 23
934      PZ = P(I)
935      PO = P(I+1)
936      PT = P(I+2)
937      XZ = X(I)
938      XO = X(I+1)
939      XT = X(I+2)
940      DO 2400 J = 1,33
941 C
942 C      *****
943 C      ***** 2.080 < XL < 2.240 *****
944 C      ***** 0.784597 < XND < 844951 *****
945 C      *****
946 C
947      XL = XL + DX
948      CALL SUBPRES (PZ,PO,PT,XZ,XO,XT,XL,XND,P2)
949      IF (M1 .LT. 0.01) THEN
950      CALL SUBINC
          (FUD,A,TO,PEX,XND,P2,DPS,RHO1,RHOV1,U1,W1,M1,
951      +M1S,DWSUM,T,SFSUM,RHO2,RHOV2,U2,W2,M2S,M2,DW,REX,REW,
952      +BETA,TW,SF,F,FBL,FBT,P1,FREX,FBLREX,FBTREX,RHOBAR,
953      +UBAR,MFFB,MFFS)
954      ESE
955      CALL SUBCOMP
          (FUD,A,TO,PEX,XND,P2,DPS,P1,RHO1,RHOV1,U1,W1,
956      +M1,M1S,DWSUM,T,SFSUM,RHO2,RHOV2,U2,W2,M2S,M2,DW,REX
          ,REW,
957      +BETA,TW,SF,F,FBL,FBT,FREX,FBLREX,FBTREX,RHOBAR,UBAR)
958      ENDIF
959      WRITE (11,5000) XND,M2
960      WRITE (12,5000) XND,REW
961      WRITE (13,5000) XND,REX
962      WRITE (14,5000) XND,P2
963      WRITE (15,5000) XND,TW
964      WRITE (16,5000) XND,F
965      WRITE (17,5000) XND,FBL
966      WRITE (18,5000) XND,RHOV2
967      WRITE (19,5000) XND,SF
968      WRITE (20,5000) XND,DW
969      WRITE (22,5000) XND,FREX
970      WRITE (23,5000) XND,FBLREX
971      WRITE (24,5000) XND,FBT
972      WRITE (25,5000) XND,FBTREX
973      IF (XND .GT. 0.799 .AND. XND .LT. 0.801) THEN
974      WRITE (9,5010)
          XND,F,REW,REX,BETA,M2,FREX,FBLREX,FBTREX
975      ENDIF
976      RHOV1 = RHOV2
977      RHO1 = RHO2

```

```

978      W1 = W2
979      M1S = M2S
980      M1 = M2
981      U1 = U2
982      P1 = P2
983 2400  CONTINUE
984      I = 25
985      PZ = P(I)
986      PO = P(I+1)
987      PT = P(I+2)
988      XZ = X(I)
989      XO = X(I+1)
990      XT = X(I+2)
991      DO 2600 J = 1,33
992 C
993 C      *****
994 C      ***** 2.245 < XL < 2.405 *****
995 C      ***** 0.846837 < XND < 0.907191 *****
996 C      *****
997 C
998      XL = XL + DX
999      CALL SUBPRES (PZ,PO,PT,XZ,XO,XT,XL,XND,P2)
1000     IF (M1 .LT. 0.01) THEN
1001     CALL SUBINC
1002     (FUD,A,TO,PEX,XND,P2,DPS,RHO1,RHOV1,U1,W1,M1,
1003     +M1S,DWSUM,T,SFSUM,RHO2,RHOV2,U2,W2,M2S,M2,DW,REX,REW,
1004     +BETA,TW,SF,F,FBL,FBT,P1,FREX,FBLREX,FBTREX,RHOBAR,
1005     +UBAR,MFFB,MFFS)
1006     ELSE
1007     CALL SUBCOMP
1008     (FUD,A,TO,PEX,XND,P2,DPS,P1,RHO1,RHOV1,U1,W1,
1009     +M1,M1S,DWSUM,T,SFSUM,RHO2,RHOV2,U2,W2,M2S,M2,DW,REX,
1010     +REW,
1011     +BETA,TW,SF,F,FBL,FBT,FREX,FBLREX,FBTREX,RHOBAR,UBAR)
1012     ENDIF
1013     WRITE (11,5000) XND,M2
1014     WRITE (12,5000) XND,REW
1015     WRITE (13,5000) XND,REX
1016     WRITE (14,5000) XND,P2
1017     WRITE (15,5000) XND,TW
1018     WRITE (16,5000) XND,F
1019     WRITE (17,5000) XND,FBL
1020     WRITE (18,5000) XND,RHOV2
1021     WRITE (19,5000) XND,SF
1022     WRITE (20,5000) XND,DW
1023     WRITE (22,5000) XND,FREX
1024     WRITE (23,5000) XND,FBLREX
1025     WRITE (24,5000) XND,FBT
1026     WRITE (25,5000) XND,FBTREX
1027     IF (XND .GT. 0.899 .AND. XND .LT. 0.901) THEN
1028     WRITE (9,5010)
1029     XND,F,REW,REX,BETA,M2,FREX,FBLREX,FBTREX

```

```

1026      ENDIF
1027      RHOV1 = RHOV2
1028      RHO1 = RHO2
1029      W1 = W2
1030      M1S = M2S
1031      M1 = M2
1032      U1 = U2
1033      P1 = P2
1034 2600  CONTINUE
1035      I = 27
1036      PZ = P(I)
1037      PO = P(I+1)
1038      PT = P(I+2)
1039      XZ = X(I)
1040      XO = X(I+1)
1041      XT = X(I+2)
1042      DO 2800 J = 1,34
1043 C
1044 C      *****
1045 C      ***** 2.410 < XL < 2.575 *****
1046 C      ***** 0.909077 < XND < 0.971316 *****
1047 C      *****
1048 C
1049      XL = XL + DX
1050      CALL SUBPRES (PZ,PO,PT,XZ,XO,XT,XL,XND,P2)
1051      IF (M1 .LT. 0.01) THEN
1052      CALL SUBINC
1053      (FUD,A,TO,PEX,XND,P2,DPS,RHO1,RHOV1,U1,W1,M1,
+M1S,DWSUM,T,SFSUM,RHO2,RHOV2,U2,W2,M2S,M2,DW,REX
,REW,
1054      +BETA,TW,SF,F,FBL,FBT,P1,FREX,FBLREX,FBTREX,RHOBAR,
1055      +UBAR,MFFB,MFFS)
1056      ELSE
1057      CALL SUBCOMP
1058      (FUD,A,TO,PEX,XND,P2,DPS,P1,RHO1,RHOV1,U1,W1,
+M1,M1S,DWSUM,T,SFSUM,RHO2,RHOV2,U2,W2,M2S,M2,DW,
REX,REW,
1059      +BETA,TW,SF,F,FBL,FBT,FREX,FBLREX,FBTREX,RHOBAR,UBAR)
1060      ENDIF
1061      WRITE (11,5000) XND,M2
1062      WRITE (12,5000) XND,REW
1063      WRITE (13,5000) XND,REX
1064      WRITE (14,5000) XND,P2
1065      WRITE (15,5000) XND,TW
1066      WRITE (16,5000) XND,F
1067      WRITE (17,5000) XND,FBL
1068      WRITE (18,5000) XND,RHOV2
1069      WRITE (19,5000) XND,SF
1070      WRITE (20,5000) XND,DW
1071      WRITE (22,5000) XND,FREX
1072      WRITE (23,5000) XND,FBLREX
1073      WRITE (24,5000) XND,FBT

```

```

1074      WRITE (25,5000) XND,FBTREX
1075      RHOV1 = RHOV2
1076      RHO1 = RHO2
1077      W1 = W2
1078      M1S = M2S
1079      M1 = M2
1080      U1 = U2
1081      P1 = P2
1082 2800  CONTINUE
1083      I = 28
1084      PZ = P(I)
1085      PO = P(I+1)
1086      PT = P(I+2)
1087      XZ = X(I)
1088      XO = X(I+1)
1089      XT = X(I+2)
1090      DO 3000 J = 1,15
1091 C
1092 C      *****
1093 C      ***** 2.580 < XL < 2.650 *****
1094 C      ***** 0.973202 < XND < 0.999607 *****
1095 C      *****
1096 C
1097      XL = XL + DX
1098      CALL SUBPRES (PZ,PO,PT,XZ,XO,XT,XL,XND,P2)
1099      IF (M1 .LT. 0.01) THEN
1100      CALL SUBINC
1101      (FUD,A,T0,PEX,XND,P2,DPS,RHO1,RHOV1,U1,W1,M1,
+M1S,DWSUM,T,SFSUM,RHO2,RHOV2,U2,W2,M2S,M2,DW,REX,
REW,
1102      +BETA,TW,SF,F,FBL,FBT,P1,FREX,FBLREX,FBTREX,RHOBAR,
+UBAR,MFFB,MFFS)
1103      ELSE
1104      CALL SUBCOMP
1105      (FUD,A,T0,PEX,XND,P2,DPS,P1,RHO1,RHOV1,U1,W1,
+M1,M1S,DWSUM,T,SFSUM,RHO2,RHOV2,U2,W2,M2S,M2,DW,
REX,REW,
1106      +BETA,TW,SF,F,FBL,FBT,FREX,FBLREX,FBTREX,RHOBAR,UBAR)
1107      ENDIF
1108      WRITE (11,5000) XND,M2
1109      WRITE (12,5000) XND,REW
1110      WRITE (13,5000) XND,REX
1111      WRITE (14,5000) XND,P2
1112      WRITE (15,5000) XND,TW
1113      WRITE (16,5000) XND,F
1114      WRITE (17,5000) XND,FBL
1115      WRITE (18,5000) XND,RHOV2
1116      WRITE (19,5000) XND,SF
1117      WRITE (20,5000) XND,DW
1118      WRITE (22,5000) XND,FREX
1119      WRITE (23,5000) XND,FBLREX
1120      WRITE (24,5000) XND,FBT
1121

```

```

1122      WRITE (25,5000) XND,FBTREX
1123      RHOV1 = RHOV2
1124      RHO1 = RHO2
1125      W1 = W2
1126      M1S = M2S
1127      M1 = M2
1128      U1 = U2
1129      P1 = P2
1130 3000  CONTINUE
1131      PI = 3.1415926536D0
1132      D = 0.5/12.0
1133      CL = (31.8125 - 16.15625)/12.0
1134      AC = PI*D**2/4.0
1135      PF = (P(1) - P(30))*AC
1136      TEST = PF - SFSUM
1137      PEF = DABS(100.0*TEST/PF)
1138      PEM = DABS(100.0*DWSUM/WCK)
1139      WRITE (9,5090) PF,TEST,PEF,WCK,DWSUM,PEM
1140      SFC = PF - SFEA
1141      TWBARC = SFC/(PI*D*CL)
1142      FBARC = 2.0*GC*TWBARC/(RHOC*UBARC**2)
1143      FCREXC = FBARC*REXBRC
1144      WRITE (9,5100) FBARC
1145      WRITE (9,5110) FCREXC
1146 C
1147 C      *****
1148 C      ***** READ FORMAT'S *****
1149 C      *****
1150 C
1151 4000  FORMAT (I1)
1152 4010  FORMAT (F15.12)
1153 4020  FORMAT (F6.2)
1154 4030  FORMAT (F5.3)
1155 C
1156 C      *****
1157 C      ***** WRITE FORMAT'S *****
1158 C      *****
1159 C
1160 5000  FORMAT (1X,F20.13,5X,F20.13)
1161 5010  FORMAT
      (2X,F4.3,2X,F8.5,2X,F9.4,2X,F9.3,3X,F6.4,2X,F8.6,
      3X,F9.5,
1162      +5X,F8.5,3X,F8.5)
1163 5011  FORMAT
      (2X,F4.3,2X,F8.5,2X,F9.4,2X,F9.3,3X,F6.4,2X,F8.6,
      3X,F9.5,
1164      +5X,F8.5)
1165 5020  FORMAT (45X,'TEST RUN # ',I1,////)
1166 5030  FORMAT (15X,'Patm      = ',F7.4,1X,'psia',/)
1167 5040  FORMAT (15X,'T0       = ',F6.2,3X,'R',/)
1168 5050  FORMAT (15X,'Psink    = ',F7.4,1X,'psia',/)
1169 5060  FORMAT (3X,'ENTER THE POROSITY FLUX CORRECTION

```

```

      FACTOR, X.XXX')
1170 5061  FORMAT (3X,'ENTER THE BLOWING MOMENTUM FLUX
      FACTOR, X.XXX')
1171 5062  FORMAT (3X,'ENTER THE SUCTION MOMENTUM FLUX
      FACTOR, X.XXX')
1172 5070  FORMAT (15X,'Porosity',/,15X,'Flux Factor =
      ',2X,F5.3,/,15X,
1173      +'Blowing Momentum',/,15X,'Flux Factor =
      ',2X,F5.3,/,15X,
1174      +'Suction Momentum',/,15X,'Flux Factor =
      ',2X,F5.3,///)
1175 5080  FORMAT
      (21X,'RADIAL',6X,'AXIAL',37X,'FB(REX)',4X,'FB(REX)'
      ,/,
1176      +3X,'X/L',2X,'FRICTION',3X,'REYNOLDS',3X,'REYNOLDS',
      5X,'BETA',
1177      +6X,'MACH',6X,'F(REX)',6X,'F. DEV.',4X,'F.
      DEV.',/,10X,'FACTOR',
1178      +5X,'NUMBER',5X,'NUMBER',13X,'NUMBER',18X,'LAMINAR'
      ,2X,
1179      +'TURBULENT',/)
1180 5090  FORMAT (///,15X,'Pressure Force',5X,'=
      ',F18.14,1X,'lbf',
1181      +/,15X,'Force Balance',6X,'=
      ',F18.14,1X,'lbf',/,15X,'% Error',
1182      +12X,'= ',F8.4,////,15X,'Mass Flow Rate',/,15X,
1183      +'Entering Condenser =
      ',F18.14,1X,'lbm/sec',/,15X,'Mass Balance',
1184      +7X,'= ',F18.14,1X,'lbm/sec',/,15X,'%
      Error',12X,'= ',F8.4)
1185 5100  FORMAT (//,15X,'Average
      Condenser',/,15X,'Friction Factor',4X,
1186      +'= ',F18.14)
1187 5110  FORMAT (//,15X,'Average Condenser',/,15X,'f(Rex)
      product',5X,
1188      +'= ',F18.14)
1189 C
1190      CLOSE (9)
1191      CLOSE (10)
1192      CLOSE (11)
1193      CLOSE (12)
1194      CLOSE (13)
1195      CLOSE (14)
1196      CLOSE (15)
1197      CLOSE (16)
1198      CLOSE (17)
1199      CLOSE (18)
1200      CLOSE (19)
1201      CLOSE (20)
1202      CLOSE (21)
1203      CLOSE (22)
1204      CLOSE (23)

```

```

1205      CLOSE (24)
1206      CLOSE (25)
1207 C
1208 C      *****
1209 C      ***** END OF MAIN PROGRAM *****
1210 C      *****
1211 C
1212      END

```

Name	Type	Offset	P	Class
A	REAL*8	1034		
AC	REAL*8	1458		
BETA	REAL*8	1298		
CL	REAL*8	1450		
D	REAL*8	1442		
DABS				INTRINSIC
DPS	REAL*8	1202		
DW	REAL*8	1274		
DWSUM	REAL*8	1130		
DX	REAL*8	1026		
F	REAL*8	1322		
FBARC	REAL*8	1514		
FBL	REAL*8	1330		
FBLREX	REAL*8	1354		
FBT	REAL*8	1338		
FBTREX	REAL*8	1362		
FCREXC	REAL*8	1522		
FREX	REAL*8	1346		
FUD	REAL*8	1002		
GC	REAL*8	1114		
I	INTEGER*4	998		
J	INTEGER*4	1386		
K	INTEGER*4	1390		
M1	REAL*8	1066		
M1S	REAL*8	1058		
M2	REAL*8	1266		
M2S	REAL*8	1258		
MFFB	REAL*8	1010		
MFFS	REAL*8	1018		
N	INTEGER*4	970		
P	REAL*8	482		
P1	REAL*8	1082		
P2	REAL*8	1090		
PATM	REAL*8	974		
PEF	REAL*8	1482		
PEM	REAL*8	1490		
PEX	REAL*8	1122		
PF	REAL*8	1466		
PI	REAL*8	1434		
PL	REAL*8	962		
PND	REAL*8	722		

PO	REAL*8	1154
PSINK	REAL*8	990
PT	REAL*8	1162
PZ	REAL*8	1146
R	REAL*8	1106
REW	REAL*8	1290
REX	REAL*8	1282
REXBRC	REAL*8	1402
RHO1	REAL*8	1210
RHO2	REAL*8	1226
RHOBAR	REAL*8	1370
RHOC	REAL*8	1418
RHOV1	REAL*8	1218
RHOV2	REAL*8	1234
SF	REAL*8	1314
SFC	REAL*8	1498
SFEA	REAL*8	1410
SFSUM	REAL*8	1138
T	REAL*8	1098
T0	REAL*8	982
TEST	REAL*8	1474
TW	REAL*8	1306
TWBARC	REAL*8	1506
U1	REAL*8	1074
U2	REAL*8	1242
UBAR	REAL*8	1378
UBARC	REAL*8	1394
W1	REAL*8	1050
W2	REAL*8	1250
WCK	REAL*8	1426
X	REAL*8	2
XL	REAL*8	1042
XND	REAL*8	1194
XNDD	REAL*8	242
XO	REAL*8	1178
XT	REAL*8	1186
XZ	REAL*8	1170

```

1213 C
1214 C *****
1215 C INTERPOLATION SUBROUTINE TO DETERMINE LOCAL PRESSURE
1216 C *****
1217 C
1218 SUBROUTINE SUBPRES (PZ,PO,PT,X7,XO,XT,XL,XND,P2)
1219 C
1220 C ** GIVEN THREE PRESSURES, PZ, PO, & PT, AT THREE
LOCATIONS,
1221 C XZ, XO, & XT, THIS SUBROUTINE INTERPOLATES
TO FIND THE
1222 C PRESSURE, P2, WITH THE REQUIREMENT XO < XL
< XT. XL IS

```



```

1223 C      REFERRED TO AS "STATION 2" **
1224 C
1225      IMPLICIT REAL*8 (A-H,O-Z)
1226      PL = 31.8125/12.0
1227      CC1 = PZ/((XZ - XO)*(XZ - XT))
1228      CC2 = PO/((XO - XZ)*(XO - XT))
1229      CC3 = PT/((XT - XZ)*(XT - XO))
1230      P2 = CC1*(XL - XO)*(XL - XT) + CC2*(XL - XZ)*(XL
1231      - XT) + CC3*(XL
1232      +- XZ)*(XL - XO)
1232      XND = XL/PL
1233      RETURN
1234      END

```

Name	Type	Offset	P	Class
------	------	--------	---	-------

CC1	REAL*8	3076		
CC2	REAL*8	3084		
CC3	REAL*8	3092		
P2	REAL*8	32	*	
PL	REAL*8	3068		
PO	REAL*8	4	*	
PT	REAL*8	8	*	
PZ	REAL*8	0	*	
XL	REAL*8	24	*	
XND	REAL*8	28	*	
XO	REAL*8	16	*	
XT	REAL*8	20	*	
XZ	REAL*8	12	*	

```

1235 C
1236 C      *****
1237 C      ***** INCOMPRESSIBLE MODEL SUBROUTINE *****
1238 C      *****
1239 C
1240      SUBROUTINE SUBINC
1241      (FUD,A,T0,PEX,XND,P2,DPS,RHO1,RHOV1,U1,W1,M1,
1242      +M1S,DWSUM,T,SFSUM,RHO2,RHOV2,U2,W2,M2S,M2,DW,REX,
1243      REW,BETA,T
1244      W,SF,
1245      +F,FBL,FBT,P1,FREX,FBLREX,FBTREX,RHOBAR,UBAR,MFFB,
1246      MFFS)
1247      ** THIS SUBROUTINE CALCULATES FLOW PROPETIES AT
1248      STATION 2 BASED ON AN INCOMPRESSIBLE MODEL **
1249      IMPLICIT REAL*8 (A-H,M,O-Z)
1250      PI = 3.1415926536D0
1251      D = 0.5/12.0
1252      DX = 0.005

```

```

1251      AP = PI*D*DX
1252      AC = PI*D**2/4.0
1253      GC = 32.174
1254      R = 53.335
1255      GAM = 1.4
1256      GAM1 = 0.2
1257      PL = 31.8125/12.0
1258      CL = (31.8125/2.0 - 0.25)/12.0
1259      DPS = P2**2 - PEX**2
1260      ADPS = DABS(DPS)
1261      RHOV2 = FUD*GC*ADPS/A
1262      IF (XND .LT. 0.5) RHOV2 = -RHOV2
1263      RHOVAV = (RHOV1 + RHOV2)/2.0
1264      DW = -RHOVAV*AP
1265      DWSUM = DWSUM + DW
1266      W2 = W1 + DW
1267      WBAR = (W1 + W2)/2.0
1268      RHO2 = P2/(R*T)
1269      RHOBAR = (RHO1 + RHO2)/2.0
1270      C2 = GC*GAM*P2/RHO2
1271      U2 = RHO1*U1/RHO2 + DW/(RHO2*AC)
1272      UBAR = (U1 + U2)/2.0
1273      M2S = U2**2/C2
1274      MSBAR = (M1S + M2S)/2.0
1275      M2 = DSQRT(M2S)
1276      CON1 = 1 + GAM1*MSBAR
1277      T = T0/CON1
1278      RMU = 2.27E-08*DSQRT(T**3)/(T + 198.6)
1279      REX = 4.0*WBAR/(PI*D*RMU*GC)
1280      REW = RHOVAV*D/(RMU*GC)
1281      BETA = DABS(REW/REX)
1282      MFF1 = MFFB
1283      MFF2 = MFFB
1284      IF (XND .GT. 0.508) MFF2 = MFFS
1285      IF (XND .GT. 0.510) MFF1 = MFFS
1286      DMOM = W2*U2*MFF2/GC - W1*U1*MFF1/GC
1287      TW = ((P1 - P2)*AC - DMOM)/AP
1288      SF = TW*AP
1289      SFSUM = SFSUM + SF
1290      F = 2.0*GC*TW/(RHOBAR*UBAR**2)
1291      AREX = DABS(REX)
1292      FBL = 16.0/REX*(1.2337 -
0.2337*DEXP(0.0363*REW))*DEXP(1.2*MSBAR)
1293      FSTAR = 0.079/AREX**0.25
1294      FBT = FSTAR*(1.0 + 17.5*AREX**0.25*BETA)
1295      FREX = F*REX
1296      FBLREX = FBL*REX
1297      FBTREX = FBT*REX
1298      IF (XND .LT. 0.491) THEN
1299      WRITE (27,6000) F,FBL
1300      ENDIF
1301 6000  FORMAT (1X,F13.9,2X,F13.9)

```

1302        RETURN  
1303        END

Name	Type	Offset	P	Class
A	REAL*8	4	*	
AC	REAL*8	3132		
ADPS	REAL*8	3188		
AP	REAL*8	3124		
AREX	REAL*8	3268		
BETA	REAL*8	100	*	
C2	REAL*8	3212		
CL	REAL*8	3180		
CON1	REAL*8	3228		
D	REAL*8	3108		
DABS				INTRINSIC
DEXP				INTRINSIC
DMOM	REAL*8	3260		
DPS	REAL*8	24	*	
DSQRT				INTRINSIC
DW	REAL*8	88	*	
DWSUM	REAL*8	52	*	
DX	REAL*8	3116		
F	REAL*8	112	*	
FBL	REAL*8	116	*	
FBLREX	REAL*8	132	*	
FBT	REAL*8	120	*	
FBTREX	REAL*8	136	*	
FREX	REAL*8	128	*	
FSTAR	REAL*8	3276		
FUD	REAL*8	0	*	
GAM	REAL*8	3156		
GAM1	REAL*8	3164		
GC	REAL*8	3140		
M1	REAL*8	44	*	
M1S	REAL*8	48	*	
M2	REAL*8	84	*	
M2S	REAL*8	80	*	
MFF1	REAL*8	3244		
MFF2	REAL*8	3252		
MFFB	REAL*8	148	*	
MFFS	REAL*8	152	*	
MSBAR	REAL*8	3220		
P1	REAL*8	124	*	
P2	REAL*8	20	*	
PEX	REAL*8	12	*	
PI	REAL*8	3100		
PL	REAL*8	3172		
R	REAL*8	3148		
REW	REAL*8	96	*	
REX	REAL*8	92	*	
RHO1	REAL*8	28	*	

RHO2	REAL*8	64 *
RHOBAR	REAL*8	140 *
RHOV1	REAL*8	32 *
RHOV2	REAL*8	68 *
RHOVAV	REAL*8	3196
RMU	REAL*8	3236
SF	REAL*8	108 *
SFSUM	REAL*8	60 *
T	REAL*8	56 *
TO	REAL*8	8 *
TW	REAL*8	104 *
U1	REAL*8	36 *
U2	REAL*8	72 *
UBAR	REAL*8	144 *
W1	REAL*8	40 *
W2	REAL*8	76 *
WBAR	REAL*8	3204
XND	REAL*8	16 *

```

1304 C
1305 C *****
1306 C ***** COMPRESSIBLE MODEL SUBROUTINE *****
1307 C *****
1308 C
1309 SUBROUTINE SUBCOMP
      (FUD,A,TO,PEX,XND,P2,DPS,P1,RHO1,RHOV1,U1,W1,
1310 +M1,M1S,DWSUM,T,SFSUM,RHO2,RHOV2,U2,W2,M2S,M2,DW,
      REX,REW,BET,A,TW,
1311 +SF,F,FBL,FBT,FREX,FBLREX,FBTREX,RHOBAR,UBAR)
1312 C
1313 C ** THIS SUBROUTINE CALCULATES FLOW PROPETIES AT
1314 C STATION 2 BASED ON A COMPRESSIBLE MODEL **
1315 C
1316 IMPLICIT REAL*8 (A-H,M,O-Z)
1317 PI = 3.1415926536D0
1318 D = 0.5/12.0
1319 DX = 0.005
1320 AP = PI*D*DX
1321 AC = PI*D**2/4.0
1322 GC = 32.174
1323 R = 53.335
1324 GAM = 1.4
1325 GAM1 = 0.2
1326 PL = 31.8125/12.0
1327 CL = (31.8125/2.0 - 0.25)/12.0
1328 DPS = P2**2 - PEX**2
1329 ADPS = DABS(DPS)
1330 RHOV2 = FUD*GC*ADPS/A
1331 IF (XND .LT. 0.5) RHOV2 = -RHOV2
1332 RHOVAV = (RHOV1 + RHOV2)/2.0
1333 DW = -RHOVAV*AP

```

```

1334      DWSUM = DWSUM + DW
1335      W2 = W1 + DW
1336      WBAR = (W1 + W2)/2.0
1337      CM = M1S*(1.0 +
      GAM1*M1S)*((W2/W1)**2)/((P2/P1)**2)
1338      M2S = (-1.0 + DSQRT(1.0 +
      4.0*GAM1*CM))/(2.0*GAM1)
1339      MSBAR = (M1S + M2S)/2.0
1340      M2 = DSQRT(M2S)
1341      CON1 = 1 + GAM1*MSBAR
1342      T = T0/CON1
1343      RHO2 = P2/(R*T)
1344      RHOBAR = (RHO1 + RHO2)/2.0
1345      C2 = GC*GAM*P2/RHO2
1346      U2 = M2*DSQRT(C2)
1347      UBAR = (U1 + U2)/2.0
1348      RMU = 2.27E-08*DSQRT(T**3)/(T + 198.6)
1349      REX = 4.0*WBAR/(PI*D*RMU*GC)
1350      REW = RHOVAV*D/(RMU*GC)
1351      BETA = DABS(REW/REX)
1352      CFP = (1.0 + GAM*MSBAR)/(GAM*MSBAR)
1353      F = 0.5*(D/DX)*(DLOG(M1S/M2S) - CFP*DLOG(P2/P1))
1354      TW = 0.5*F*RHOBAR*UBAR**2/GC
1355      SF = TW*AP
1356      SFSUM = SFSUM + SF
1357      AREX = DABS(REX)
1358      FBL = 16.0/REX*(1.2337 -
      0.2337*DEXP(0.0363*REW))*DEXP(1.2*MSBAR)
1359      FSTAR = 0.079/AREX**0.25
1360      FBT = FSTAR*(1.0 + 17.5*AREX**0.25*BETA)
1361      FREX = F*REX
1362      FBLREX = FBL*REX
1363      FBTREX = FBT*REX
1364      IF (XND .LT. 0.491) THEN
1365      WRITE (27,6000) F,FBL
1366      ENDIF
1367 6000  FORMAT (1X,F13.9,2X,F13.9)
1368      RETURN
1369      END

```

Name	Type	Offset	P	Class
A	REAL*8		4	*
AC	REAL*8	3336		
ADPS	REAL*8	3392		
AP	REAL*8	3328		
AREX	REAL*8	3464		
BETA	REAL*8	104	*	
C2	REAL*8	3440		
CFP	REAL*8	3456		
CL	REAL*8	3384		
CM	REAL*8	3416		

CON1	REAL*8	3432	
D	REAL*8	3312	
DABS			INTRINSIC
DEXP			INTRINSIC
DLOG			INTRINSIC
DPS	REAL*8	24	*
DSQRT			INTRINSIC
DW	REAL*8	92	*
DWSUM	REAL*8	56	*
DX	REAL*8	3320	
F	REAL*8	116	*
FBL	REAL*8	120	*
FBLREX	REAL*8	132	*
FBT	REAL*8	124	*
FBTREX	REAL*8	136	*
FREX	REAL*8	128	*
FSTAR	REAL*8	3472	
FUD	REAL*8	0	*
GAM	REAL*8	3360	
GAM1	REAL*8	3368	
GC	REAL*8	3344	
M1	REAL*8	48	*
M1S	REAL*8	52	*
M2	REAL*8	88	*
M2S	REAL*8	84	*
MSBAR	REAL*8	3424	
P1	REAL*8	28	*
P2	REAL*8	20	*
PEX	REAL*8	12	*
PI	REAL*8	3304	
PL	REAL*8	3376	
R	REAL*8	3352	
REW	REAL*8	100	*
REX	REAL*8	96	*
RHO1	REAL*8	32	*
RHO2	REAL*8	68	*
RHOBAR	REAL*8	140	*
RHOV1	REAL*8	36	*
RHOV2	REAL*8	72	*
RHOVAV	REAL*8	3400	
RMU	REAL*8	3448	
SF	REAL*8	112	*
SFSUM	REAL*8	64	*
T	REAL*8	60	*
T0	REAL*8	8	*
TW	REAL*8	108	*
U1	REAL*8	40	*
U2	REAL*8	76	*
UBAR	REAL*8	144	*
W1	REAL*8	44	*
W2	REAL*8	80	*
WBAR	REAL*8	3408	

XND      REAL\*8                      16 \*

Name	Type	Size	Class
ONED			PROGRAM
SUBCOM			SUBROUTINE
SUBINC			SUBROUTINE
SUBPRE			SUBROUTINE

Pass One      No Errors Detected  
                 1369 Source Lines

Appendix C

TEST RUN # 1

Patm = 14.2827 psia

T0 = 526.50 R

Psink = 14.2444 psia

Porosity  
Flux Factor = 1.000

Blowing Momentum  
Flux Factor = 1.290

Suction Momentum  
Flux Factor = 1.470

X/L	FRICTION FACTOR	RADIAL REYNOLDS NUMBER	AXIAL REYNOLDS NUMBER	BETA	MACH NUMBER	F (REX)
.100	.18663	-3.4595	87.995	.0393	.000312	16.42282
.200	.09210	-3.4621	176.035	.0197	.000625	16.21332
.300	.06123	-3.4665	264.163	.0131	.000938	16.17488
.400	.04737	-3.4726	352.423	.0099	.001251	16.69325
.600	.03083	3.4723	354.203	.0098	.001252	10.91849
.700	.05958	3.4734	265.850	.0131	.000938	15.84048
.800	.08847	3.4740	177.478	.0196	.000624	15.70187
.900	.12791	3.4745	89.092	.0390	.000310	11.39598

Pressure Force = .00001883160918 lbf

Force Balance = .00000000005909 lbf

% Error = .0003

Mass Flow Rate  
Entering Condenser = .00017256225293 lbm/sec

Mass Balance = -.00000005382849 lbm/sec

% Error = .0312

Average Condenser  
Friction Factor = .06447082216418

Average Condenser  
f(Rex) product = 13.99607226000200



# TEST RUN # 2

Patm = 14.2484 psia

T0 = 526.00 R

Psink = 14.2281 psia

Porosity  
Flux Factor = 1.000

Blowing Momentum  
Flux Factor = 1.305

Suction Momentum  
Flux Factor = 1.370

X/L	FRICTION FACTOR	RADIAL REYNOLDS NUMBER	AXIAL REYNOLDS NUMBER	BETA	MACH NUMBER	F(REX)
.100	.34820	-1.8347	46.669	.0393	.000166	16.24985
.200	.17400	-1.8357	93.355	.0197	.000332	16.24329
.300	.11622	-1.8375	140.076	.0131	.000498	16.27910
.400	.08698	-1.8399	186.850	.0098	.000664	16.25176
.600	.08404	1.8414	187.725	.0098	.000664	15.77694
.700	.11145	1.8409	140.887	.0131	.000497	15.70123
.800	.16664	1.8405	94.061	.0196	.000331	15.67422
.900	.33160	1.8403	47.242	.0390	.000165	15.66552

Pressure Force = .00001122276190 lbf

Force Balance = .000000000000089 lbf

% Error = .0000

Mass Flow Rate  
Entering Condenser = .00009140706303 lbm/sec

Mass Balance = -.000000000598701 lbm/sec

% Error = .0065

Average Condenser  
Friction Factor = .13496525522116

Average Condenser  
f(Rex) product = 15.53163701557668

TEST RUN # 3

Patm = 14.3022 psia

T0 = 526.00 R

Psink = 14.2308 psia

Porosity  
Flux Factor = 1.000

Blowing Momentum  
Flux Factor = 1.270

Suction Momentum  
Flux Factor = 1.600

X/L	FRICTION FACTOR	RADIAL REYNOLDS NUMBER	AXIAL REYNOLDS NUMBER	BETA	MACH NUMBER	F (REX)
.100	.10239	-6.4532	164.129	.0393	.000582	16.80494
.200	.05118	-6.4602	328.378	.0197	.001164	16.80719
.300	.03387	-6.4720	492.866	.0131	.001747	16.69245
.400	.02542	-6.4885	657.713	.0099	.002332	16.72037
.600	.02416	6.4716	661.560	.0098	.002334	15.98275
.700	.02319	6.4815	496.794	.0130	.001750	11.52303
.800	.04039	6.4884	331.809	.0196	.001165	13.40302
.900	.06137	6.4937	166.669	.0390	.000580	10.22789

Pressure Force = .00002995839503 lbf

Force Balance = .00000000004151 lbf

% Error = .0001

Mass Flow Rate  
Entering Condenser = .00032190622080 lbm/sec

Mass Balance = -.00000002620157 lbm/sec

% Error = .0081

Average Condenser  
Friction Factor = .03506096928445

Average Condenser  
f(Rex) product = 14.20926769146199

# TEST RUN # 4

Patm = 14.2729 psia

T0 = 526.00 R

Psink = 14.1330 psia

Porosity

Flux Factor = 1.000

Blowing Momentum

Flux Factor = 1.245

Suction Momentum

Flux Factor = 1.600

X/L	FRICTION FACTOR	RADIAL REYNOLDS NUMBER	AXIAL REYNOLDS NUMBER	BETA	MACH NUMBER	F (REX)
.100	.05462	-12.5627	319.471	.0393	.001138	17.45062
.200	.02702	-12.5848	639.317	.0197	.002277	17.27199
.300	.01815	-12.6219	959.915	.0131	.003418	17.41907
.400	.01360	-12.6740	1281.648	.0099	.004564	17.43204
.600	.01261	12.5920	1290.864	.0098	.004575	16.27655
.700	.01401	12.6353	969.950	.0130	.003432	13.58974
.800	.02095	12.6676	648.078	.0195	.002286	13.57851
.900	.12140	12.6756	325.702	.0389	.001138	39.54022

Pressure Force = .00005293412287 lbf

Force Balance = .00000000069008 lbf

% Error = .0013

Mass Flow Rate

Entering Condenser = .00062766683506 lbm/sec

Mass Balance

= .00000004480944 lbm/sec

% Error

= .0071

Average Condenser

Friction Factor = .02606307347730

Average Condenser

f(Rex) product = 20.59576260070104

### Bibliography

1. Berman, A. S. "Effects of Porous Boundaries on the Flow of Fluids in Systems with Various Geometries," Proceedings of the Second United Nations International Conference on the Peaceful Uses of Atomic Energy, Vol. 4, pp. 351-358, United Nations, Geneva (1958).
2. Kinney, R. B. "Fully Developed Frictional and Heat Transfer Characteristics of Laminar Flow in Porous Tubes," International Journal of Heat and Mass Transfer, Vol. 11, pp. 1393-1401, 1968.
3. Bundy, R. D. and Weissberg, H. L. "Experimental Study of Fully Developed Laminar Flow in a Porous Pipe with Wall Injection," The Physics of Fluids, Vol. 13, No. 10, pp. 2613-2615, October 1970.
4. Gupta, R. C. "Laminar Flow in the Inlet Region of a Porous Tube," Applied Science Research, Vol. 22, pp. 360-365, July 1970.
5. Bowman, Capt W. J. Heat Pipe Vapor Dynamics. PhD Dissertation, School of Engineering, Air Force Institute of Technology (AU), Wright-Patterson AFB OH, May 1987 (88182592).
6. Weissberg, H. L. "Laminar Flow in the Entrance Region of a Porous Pipe," The Physics of Fluids, Vol. 2, No. 5, pp. 510-516, September-October 1959.
7. Raithby, G. "Laminar Heat Transfer in the Thermal Entrance Region of Circular Tubes and Two-Dimensional Rectangular Ducts with Wall Suction and Injection," International Journal of Heat and Mass Transfer, Vol. 14, pp. 223-243, 1971.
8. Hornbeck, R. W., Rouleau, W. T., and Osterle, F. "Laminar Entry Problem in Porous Tubes," The Physics of Fluids, Vol. 6, No. 11, pp. 1649-1654, November 1963.
9. Quaile, J. P. and Levy, E. K. "Laminar Flow in a Porous Tube With Suction," Journal of Heat Transfer. Transactions of the ASME, pp. 66-71, February 1975.
10. Wageman, W. E. and Guevara, F. A. "Fluid Flow Through a Porous Channel," The Physics of Fluids, Vol. 3, No. 6, pp. 878-881, November-December 1960.

11. Kinney, R. B. and Sparrow, E. M. "Turbulent Flow, Heat Transfer, and Mass Transfer in a Tube With Surface Suction," Journal of Heat Transfer. Transactions of the ASME, pp. 117-125, February 1970.
12. Muskat, M. The Flow of Homogeneous Fluids Through Porous Media, J. W. Edwards, Inc. Ann Arbor, Michigan, 1946.
13. Holladay, C. A. Compressible Friction Coefficients in a Simulated Heat Pipe. MS Thesis AFIT/GAE/AA/87D-6. School of Engineering, Air Force Institute of Technology (AU), Wright-Patterson AFB OH, December 1987.
14. Shapiro, A. H. The Dynamics and Thermodynamics of Compressible Fluid Flow. Vol. 1, pp. 231-239, The Ronald Press Company, New York, 1953.

Vita

Captain David A. Manley [REDACTED]

[REDACTED] He graduated from high school in Big Spring, Texas, in 1979 and attended the United States Air Force Academy, from which he received the degree of Bachelor of Science in Engineering Mechanics in May 1983. Upon graduation, he received a regular commission in the USAF. He served as a Shuttle spacecraft systems engineer and a Titan IV payload launch integration manager until entering the School of Engineering, Air Force Institute of Technology, in May 1987.

[REDACTED]

[REDACTED]

UNCLASSIFIED

SECURITY CLASSIFICATION OF THIS PAGE

REPORT DOCUMENTATION PAGE				Form Approved OMB No. 0704-0188	
1a. REPORT SECURITY CLASSIFICATION <b>UNCLASSIFIED</b>			1b. RESTRICTIVE MARKINGS		
2a. SECURITY CLASSIFICATION AUTHORITY			3. DISTRIBUTION / AVAILABILITY OF REPORT Approved for public release; distribution unlimited.		
2b. DECLASSIFICATION / DOWNGRADING SCHEDULE					
4. PERFORMING ORGANIZATION REPORT NUMBER(S) AFIT/GAE/AA/88D-22			5. MONITORING ORGANIZATION REPORT NUMBER(S)		
6a. NAME OF PERFORMING ORGANIZATION School of Engineering		6b. OFFICE SYMBOL (if applicable) AFIT/ENY	7a. NAME OF MONITORING ORGANIZATION		
6c. ADDRESS (City, State, and ZIP Code) Air Force Institute of Technology Wright-Patterson AFB OH 45433-6583			7b. ADDRESS (City, State, and ZIP Code)		
8a. NAME OF FUNDING / SPONSORING ORGANIZATION		8b. OFFICE SYMBOL (if applicable)	9. PROCUREMENT INSTRUMENT IDENTIFICATION NUMBER		
8c. ADDRESS (City, State, and ZIP Code)			10. SOURCE OF FUNDING NUMBERS		
			PROGRAM ELEMENT NO.	PROJECT NO.	TASK NO.
					WORK UNIT ACCESSION NO.
11. TITLE (Include Security Classification) INCOMPRESSIBLE FLOW FRICTION COEFFICIENTS IN A SIMULATED HEAT PIPE					
PERSONAL AUTHOR(S) David A. Manley, B.S., Capt, USAF					
13a. TYPE OF REPORT MS Thesis		13b. TIME COVERED FROM _____ TO _____		14. DATE OF REPORT (Year, Month, Day) 1988 December	
15. PAGE COUNT 96					
16. SUPPLEMENTARY NOTATION					
17. COSATI CODES			18. SUBJECT TERMS (Continue on reverse if necessary and identify by block number)		
FIELD	GROUP	SUB-GROUP			
20	04		Heat Pipe, Porous Pipe, friction factor, friction coefficient Blowing, Suction, Injection, Extraction. (JES) ←		
19. ABSTRACT (Continue on reverse if necessary and identify by block number)					
Thesis Advisor: Dr. James E. Hitchcock Professor of Mechanical Engineering					
ABSTRACT ON BACK					
DISTRIBUTION / AVAILABILITY OF ABSTRACT <input checked="" type="checkbox"/> UNCLASSIFIED/UNLIMITED <input type="checkbox"/> SAME AS RPT. <input type="checkbox"/> DTIC USERS			21. ABSTRACT SECURITY CLASSIFICATION UNCLASSIFIED		
22a. NAME OF RESPONSIBLE INDIVIDUAL Dr. James E. Hitchcock, Professor			22b. TELEPHONE (Include Area Code) (513) 255-3517		22c. OFFICE SYMBOL AFIT/ENY

DD Form 1473, JUN 86

Previous editions are obsolete.

SECURITY CLASSIFICATION OF THIS PAGE

UNCLASSIFIED

UNCLASSIFIED

19. This thesis examines the combined effects of pressure gradients and blowing and suction on frictional forces in a heat pipe with relatively low radial Reynolds numbers. A porous tube is used to simulate the heat pipe and a vacuum pump is used to generate the air flow. By measuring the static pressure variation along the pipe wall and using a one-dimensional, incompressible, numerical model, the frictional forces are obtained and compared to laminar fully-developed theoretical values. Four flow rate cases with radial Reynolds numbers of 1.8, 3.5, 6.5, and 12.6 were studied. In this range, the flow in the evaporator was fully-developed. In the condenser, however, the fully-developed solution consistently under predicted the average condenser friction coefficient. Deviation from the fully-developed solution increased as the flow rate increased.

→ *keyword* →

UNCLASSIFIED

END